Desalination and Water Treatment
www.deswater.com
doi: 10.5004/dwt.2021.27206

224 (2021) 367–388
June

Utilization of low-cost bio-waste adsorbent for methylene blue dye removal from aqueous solutions and optimization of process variables by response surface methodology approach

Pelin Yilmaz, Davut Gunduz, Belma Ozbek*

Chemical Engineering Department, Yildiz Technical University, Davutpasa Campus, Esenler, Istanbul 34220, Turkey, Tel. +90 212 3834729; emails: bozbek@yildiz.edu.tr (B. Ozbek), pyilmaz@yildiz.edu.tr (P. Yilmaz), dvtgndz@gmail.com (D. Gunduz)

Received 14 September 2020; Accepted 4 March 2021

ABSTRACT

In the present study, the sesame seed cake was utilized as an adsorbent to remove methylene blue which is one of the most used cationic dyes in various industries. The proper design of experiments conducted to adsorb methylene blue dye on sesame seed cake was carried out by using response surface methodology, Box–Behnken design. The adsorption experiments were carried out for 25 min using the initial concentration of methylene blue solution of 200 mg/L at various temperatures (20°C–40°C), pH (3–9), and adsorbent dosage values (1–3 g/100 mL). The results obtained from the adsorption experiments were evaluated by using an analysis of variance, and the statistically significant quadratic model was developed. The possible functional groups and morphological structure of sesame seed cake before and after the adsorption process was revealed by using Fourier transform infrared, Brunauer–Emmet–Teller, and scanning electron microscopy with energy-dispersive X-ray spectroscopy analysis. The comprehensive investigations about the adsorption kinetic, isotherm, thermodynamic, and reusability studies were performed to enlighten the possible adsorption mechanism of methylene blue on sesame seed cake. The various adsorption kinetic and isotherm models were examined for the data obtained from the adsorption experiments at optimum methylene blue dye removal. The data obtained from the adsorption studies indicated that the methylene blue removal on sesame seed cake fit the pseudo-second-order kinetic model and Freundlich adsorption isotherm. Thermodynamic analysis pointed that the adsorption had an endothermic nature and spontaneous at all studied temperatures. Eventually, the findings obtained from the present study indicated that the sesame seed cake is an efficient adsorbent for removing methylene blue dye from aqueous solutions in a dramatically short time with a reusability performance of three times.

Keywords: Methylene blue; Sesame seed cake; Adsorption; Response surface methodology; Box–Behnken design; Adsorption isotherm model; Adsorption kinetic model; Thermodynamic analysis; Reusability performance

1. Introduction

The high living standards, consumer demand, and rapid expansion of the industrial sector have triggered the increase of emerging contaminants and long-term exposure of them [1–3]. Thus, environmental pollution concern has become more crucial due to its undesirable impact on public health [1]. The emerging contaminants such as extensively used synthetic components (pesticides, pharmaceuticals, dyes, and personal products) are commonly present in effluents coming from different industries, such as; textile, pulp and paper, paint, cosmetic, rubber, plastic, food, pharmaceuticals, etc., using dyes to the color of their products and they also consume a substantial amount of water. [2].

* Corresponding author.

As a result, the effluents from these industries contain a considerable amount of dye that could lead to water pollution if they leak into the environment without any proper treatment [4–8]. Besides, the complex aromatic structure of dyes [9–11] makes them highly stable and hardly biodegradable [12] in an aquatic environment. Thus, the presence of them, even less than 1 ppm amount of dye in water, is highly visible and also undesirable for daily usage [7,13]. The reduction of sunlight transmission through water and dependently impaired photosynthesis, inhibition of biota [13,14], increasing the toxicity [9,15–17] are the catastrophic and undeniable consequences of the discharge of effluents containing a considerable amount of dye to the aquatic environment without any proper treatment [3,5,13]. At this point, proper treatment of aqueous solutions discharged from mentioned industries has become a crucial requirement since they triggered to increase the availability of the dyes in the aquatic environment.

Methylene blue is one of the thiazine cationic dyes containing three water molecules in the hydrating form [18–21], and it has a large variety of usage in various applications in mostly dyeing industries and sometimes medical science applications as an antidote [18,20]. Since the large application area of methylene blue in various industries, the effluents discharged could include a considerable amount of methylene blue. The long-term exposure of methylene blue has hazardous effects on humans such as increased heart rate, vomiting, hypertension [11], and some chemical compounds derived from methylene blue degradation such as toluidine and benzidine cause undesirable changes in the body [18]. Therefore, the removal of methylene blue has great importance when its wide application area, stability, and hazardous effects were considered. For the treatment of the effluents including methylene blue or any other dye compounds, various methods are preferred such as; adsorption, precipitation, fluctuations, ion exchange, electro-kinetic coagulation, ozonation [1,6,18,22], evaporation [23], distillation [23], and photodegradation [24]. Among the methods mentioned, the adsorption process is a preferred method due to its cheapness, eco-friendliness, effectiveness, and easy application [20,25,26], especially if the adsorbent is readily available [1].

The efficiency of the adsorption process mainly depends on the nature of the adsorbent (specific surface area, pore size distribution, and presence of functional groups on the surface [27]) and also dye (anionic or cationic nature [27]), and interaction between the adsorbent and adsorbate. Using an adsorbent that is efficient, low-cost, eco-friendly, etc., is a critical issue that determines the efficiency of the adsorption. Therefore, the usage of agricultural by-products as an efficient adsorbent is an economical and applicable approach for the adsorption process which is affected by the various operational conditions such as pH, temperature, adsorbent dosage, initial concentration of the dye, contact time, and the interaction of these process variables in a nonlinear way. Since there are many variables in the adsorption studies, the classical methods for process optimization are deficient to understand the interactive effects of the process variables and also time-consuming due to requiring a significant number of experiments [28,29]. To overcome these limitations, the statistical tools designing the experiments arise as an efficient approach to reduce the required experimental runs and also for time-saving [4].

Response surface methodology (RSM) is a combination of statistical methods designing the limited number of experiments sufficient to understand the interaction of the process variables, establish the mathematical models describing the process behavior [5,30–32]. In this way, the effects of process variables on the response are determined over a wide range of conditions with a minimum amount of resources. In principle, this approach includes some major steps such as (i) suggesting statistically important experimental trials and performing them, (ii) finding the actual response values and estimating the mathematical model describing the process, (iii) prediction of the response values by using the suggested mathematical model, and (iv) finally evaluation of the adequacy of the suggested model [33]. RSM provides the optimum conditions satisfying the operating specifications suggested by various designs such as BBD, central composite design, Doehlert design, etc. [30,34,35]. Box–Behnken design (BBD) is a three-level factorial design and the number of experiments is minimized in the quadratic model fitting [30]. It is the most common design approach for adsorption studies due to the reduction of experiment trials [36]. The experimental trials in BBD are arranged at just only three-levels which are equally spaced intervals between these levels and the replicated center points [36,37].

For methylene blue removal from aqueous solutions, the various studies were performed using the agricultural wastes such as rosewood sawdust [38], neem leaf powder [39], wheat shells [40], bamboo-based activated carbon [17], activated carbon prepared from rattan sawdust [11], activated carbon prepared from sunflower oil cake [41], spent coffee grounds [14], pineapple peel powder [42], Tunisian activated carbon [43], activated carbon produced from flamboyant pods [19], activated carbon prepared from *Posidonia oceanica* dead leaves [27], activated carbon prepared from cashew nut shell [44], aspapaya leaf powder [45], *Parthenium hysterophorus* [4], pine tree leaves [8], field debris of chickpea [46], activated carbon prepared from pineapple [47], corn husk [48], oil palm leaves [21], activated carbon produced from *Ficus carica* bast [20], walnut shells powder [1], corncob [49], ginger straw waste derived porous carbons [50], activated carbon prepared from *Citrus limetta* peels [51], and silica derived from the raw rice husk [52].

In the present study, sesame seed cake, which is an agricultural waste remaining from the sesame oil production process, was used as an adsorbent to remove the methylene blue from aqueous solutions. Even though there are many studies performed on methylene blue adsorption as mentioned, to the best of our knowledge, no study has been found dealing with the optimization of methylene blue adsorption on sesame seed cake by using RSM BBD. Additionally, the novelty of this paper lies in the effective utilization of almost non-valuable agricultural residue as an inexpensive adsorbent without applying any pretreatment techniques. Moreover, the data obtained from the adsorption studies suggested that the adsorbent used provided the significant uptake of targeted methylene blue dye, which is one of the most available cationic dye in aqueous solution in a dramatically short time. In this perspective, firstly, the structural, chemical, and morphological properties of

the sesame seed cake were comprehensively investigated. Then, adsorption experiments were designed using a Design Expert 11.0 trial software experimental design program, and one of the RSM members, three-level factorial BBD, was used to evaluate the interaction parameters of methylene blue adsorption on sesame seed cake. The temperature interval was arranged between 20°C and 40°C, the pH interval was arranged between 3 and 9, and the adsorbent dosage range was determined between 1 and 3 g/100 mL. These three-independent process variables were used, and 17 experiments with five replicates at the center point were conducted to reveal the effect of each variable on methylene blue removal efficiency of sesame seed cake. The initial methylene blue dye concentration and contact time were kept constant, and data collected from the experiment sets were used to fit a mathematical model for the whole process. The adequacy of the suggested mathematical model was evaluated by the analysis of variance (ANOVA). Additionally, adsorption kinetic models, adsorption isotherm models, thermodynamic and activation energy parameters, and reusability performance of sesame seed cake were examined to enlighten possible adsorption process mechanism of methylene blue onto low-cost bio-waste agricultural absorbent without any pretreatment applications.

2. Materials and Method

2.1. Materials

Methylene blue (MB) purchased by Gunduz Chemistry firm with 52015 color index in Turkey, was used as an adsorbent. Sesame seed cake supplied from Gordes agriculture firm in Turkey was used as an adsorbate. An oven (Memmert mark, 53 L) was used to dry the sesame seed cake. Sodium hydroxide (NaOH), hydrochloric acid (HCl), and ethanol were purchased Merck (Darmstadt, Germany) firm was used for pH adjustment of aqueous dye solutions with Hanna HI 2211 pH/ORP meter. The samples containing sesame seed cake and dye were agitated in an orbital shaker IKA KS 3000i. The samples withdrawn at defined time intervals were centrifuged by using HETTICH 120 micro-centrifuge. The absorbance values of residual methylene blue in the aqueous solutions were measured by using SHIMADZU UV-1800 spectrophotometer (Kyoto, Japan).

2.2. Preparation of Adsorbent

Sesame seed cake was dried at 50°C for 24 h for removing the humidity of the adsorbate in an oven. Then, it was ground. The average particle size of the cake was found as an average of 100 mesh.

2.3. Design of experiments

The operational parameters affecting the methylene blue adsorption process were optimized using RSM. This method could be defined as a collection of mathematical and statistical methods that are useful to design the experiments, develop the models fitting with the experimental results and optimize the process parameters. In the present study, a three-level factorial BBD was used to examine the interaction parameters and to predict the optimum process conditions for methylene blue removal. Principally, the number of experiments for BBD is determined by $N = 2k(k - 1) + c_p$ (k is the number of independent variables and c_p is replicated at the center point) and all factor levels must be adjusted only at three levels (low, center, and high) with equally spaced intervals between these levels [36].

In the present study, three independent process variables were determined as temperature (X_1), pH (X_2), and adsorbent dosage (X_3). According to BBD, the total number of experiments conducted was 17 with 5 replicates at the center point, to verify the effect of these three independent variables on the methylene blue removal efficiency from aqueous solutions (response: R_1). The other parameters such as contact time and initial methylene blue dye concentration were kept constant at 25 min and 200 ppm (mg/L), respectively. The response values obtained from the experimental trials were used for fitting the mathematical model describing the relationship of response values with the independent variables. The experimental design suggested by BBD was presented in Table 1.

Design-Expert 11 (State-Ease, Inc. Minneapolis, USD) software was used to fit the appropriate mathematical model, analysis of data and evaluate the statistical significance of the suggested model. An ANOVA, which is the collection of mathematical functions and statistical methods, was used to determine the accuracy of the fitted model, statistically significant parameters affecting the response and which one was the most significant.

2.4. Adsorption experiments

The methylene blue dye solution was prepared by dissolving the defined amount of methylene blue dye powder in distilled water to obtain a concentration of 1,000 mg/L methylene blue stock solution. Then, this solution was diluted to achieve 200 mg/L initial methylene blue dye concentration to be used for each experiment.

The adsorption experiments designed by RSM-BBD were carried out by mixing the defined amount of adsorbent dosage with 100 mL methylene blue solution under 150 rpm constant stirring at a defined temperature

Table 1
Experimental levels in Box–Behnken design

Factors	Levels		
	Low (–1)	Center (0)	High (+1)
A: Temperature (°C)	20	30	40
B: pH	3	6	9
C: Adsorbent dosage (g/100mL)	1	2	3

and pH range in an orbital shaker for 25 min (Table 1). The samples were withdrawn at defined time intervals and then centrifuged at 12,000 rpm for 4 min to remove the adsorbent from the solution. The residual methylene blue concentrations were calculated by using absorbance values of samples measured with a UV-spectrophotometer at 664 nm wavelength. The methylene blue removal percentage and the adsorption capacities were calculated by using the following equations:

Removal percentage,

$$R(\%) = \left(\frac{C_0 - C_t}{C_0}\right) \times 100 \quad (1)$$

Adsorption capacity at any time,

$$q_t = \frac{(C_0 - C_t)V}{M} \quad (2)$$

Adsorption capacity at equilibrium,

$$q_e = \frac{(C_0 - C_e)V}{M} \quad (3)$$

where C_0, C_t, and C_e are representing methylene blue dye concentration at the time is equal to zero, any t, and at equilibrium, respectively. V is the volume of the dye solution, and M is the weight of the adsorbent used. The results were expressed as an average of three replicates with less than ±5% standard error.

2.5. Characterization studies

Zeiss EVO LS10 scanning electron microscopy (SEM) operating in beam mode at 20 kV with a secondary electron detector was used to characterize the porous texture of sesame seed cake. Additionally, the elemental mapping and elemental composition of sesame seed cake before and after the adsorption was studied using energy dispersive X-ray spectroscopy (EDX). Bruker (Billerica, USD) Tensor 27 attenuated total reflection (ATR) Fourier-transform infrared (FTIR) spectrometer was used to observe the present functional groups on the surface of the sesame seed cake. The analysis was performed at room temperature and 600–4,000 cm^{-1} wavelength range. Quantachrome Quadrosorb SI analyzer was used to find the specific surface area of the sesame seed cake and Brunauer–Emmet–Teller (BET) analysis method was used. For the measurements; the samples were degassed at 120°C for 3 h and the analysis was applied at 77 K.

The point of zero charge (pH_{PZC}) determination of sesame seed cake was assessed by pH difference method as described in previous work [53]. According to this method, a series of nine tubes were filled with 20 mL of 0.01 M NaCl solution and then, the initial pH (pH_i) of each tube was correctly fixed at 2–10 pH values. Afterward, 0.05 g of sesame seed cake was transferred to each tube and stirred at 20°C for 5 h. The final pH (pH_f) values of each tube were determined with Hanna HI 2211 pH/ORP meter. The intersection point of the curve of ΔpH (pH_f – pH_i) vs. pH_i with the pH_i axis represents the pH_{PZC} value of the sesame seed cake. The measurements were replicated three times and the results were expressed as an average with ±5% reproducibility of the measurement.

3. Results and discussions

3.1. Characterization studies on sesame seed cake

The morphological structure of sesame seed cake before and after the adsorption process was observed by SEM analysis and the images at the magnifications of 5.00 and 10.00 KX are represented in Figs. 1a and b, respectively.

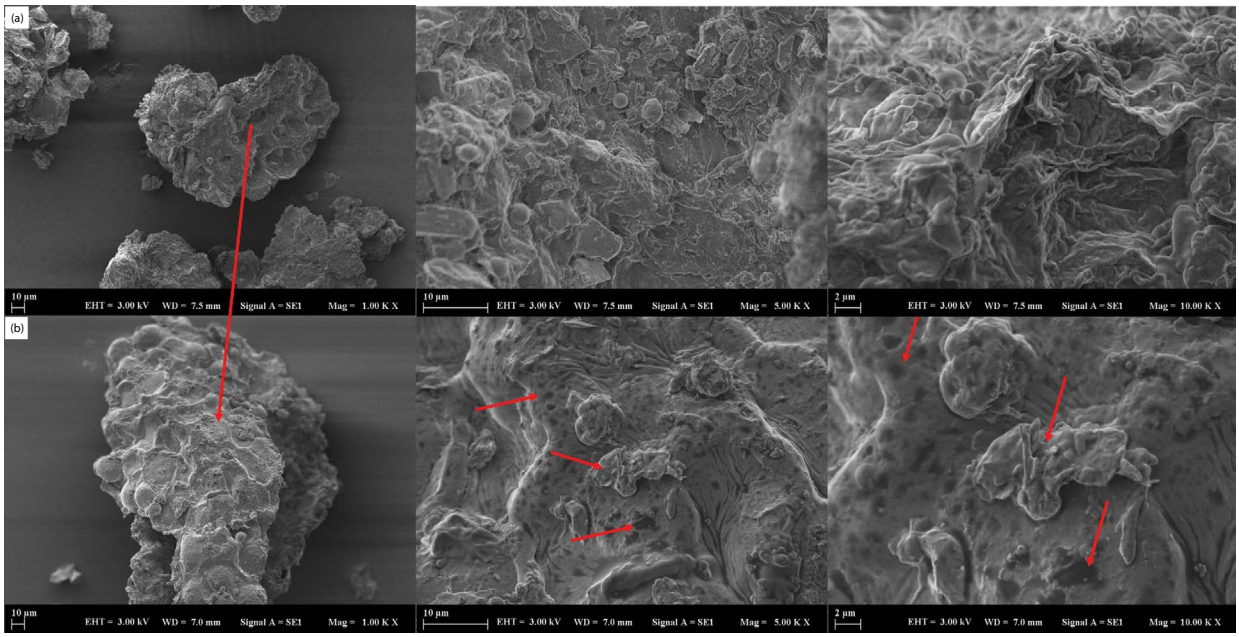

Fig. 1. SEM images of sesame seed cake (a) before and (b) after adsorption process at 1.00, 5.00, and 10.00 KX magnifications.

According to the results obtained, the amorphous nature and irregular cubic morphology with heterogeneous pore distribution of sesame seed cake were observed before the methylene blue adsorption. After the adsorption process, the smooth surface of the sesame seed cake had become rougher since the methylene blue covered the surface of the sesame seed cake and diffused inside the pores. If the images are carefully examined, it will be noticed that the pores present on the surface of the sesame seed cake had become darker. The underlying reason for this situation could be explained by the diffusion of methylene blue dye inside the pores (as shown in Fig. 1b). Additionally, apart from the diffusion inside the pores, the methylene blue coverage on the external surface of the sesame seed cake was clearly observed. The functional groups which were enlightened by FTIR analysis were responsible active sites that interacted with methylene blue dye.

The elemental mapping and composition of sesame seed cake before and after the adsorption process are given in Fig. 2. The results showed that the surface of sesame seed cake mainly consists of carbon, oxygen, and nitrogen elements at a significant percentage compared to other elements such as magnesium, sulfur, potassium, and calcium (Fig. 2a) and the distribution of these elements at the selected area are given in Fig. 2b. The distribution of the present elements confirmed that while the backbone of the sesame seed cake mainly consists of carbon, the oxygen, and nitrogen elements expanded through the carbon backbone. These elements were mainly responsible to form the functional groups playing a role in the methylene blue adsorption.

The EDX analysis of sesame seed cake before and after the adsorption of methylene blue was found as quite similar. It was found that the sesame seed cake and methylene blue had similar elemental composition. In Fig. 2c, the elemental composition of sesame seed cake after the methylene blue adsorption is given. According to the results obtained, it was observed that sulfur and nitrogen presence at the selected area increased possibly due to the surface coverage by methylene blue. After the adsorption process, the distribution of the nitrogen and oxygen elements changed since these elements were responsible to form the hydrogen bonds between the sesame seed cake surface and methylene blue (Fig. 2d).

The FTIR analysis was performed to identify the possible functional groups of sesame seed cake involved in methylene blue adsorption. In Fig. 3, FTIR spectra of sesame seed cake before and after adsorption of methylene blue are given. According to the results obtained for FTIR analysis of sesame seed cake before methylene blue adsorption,

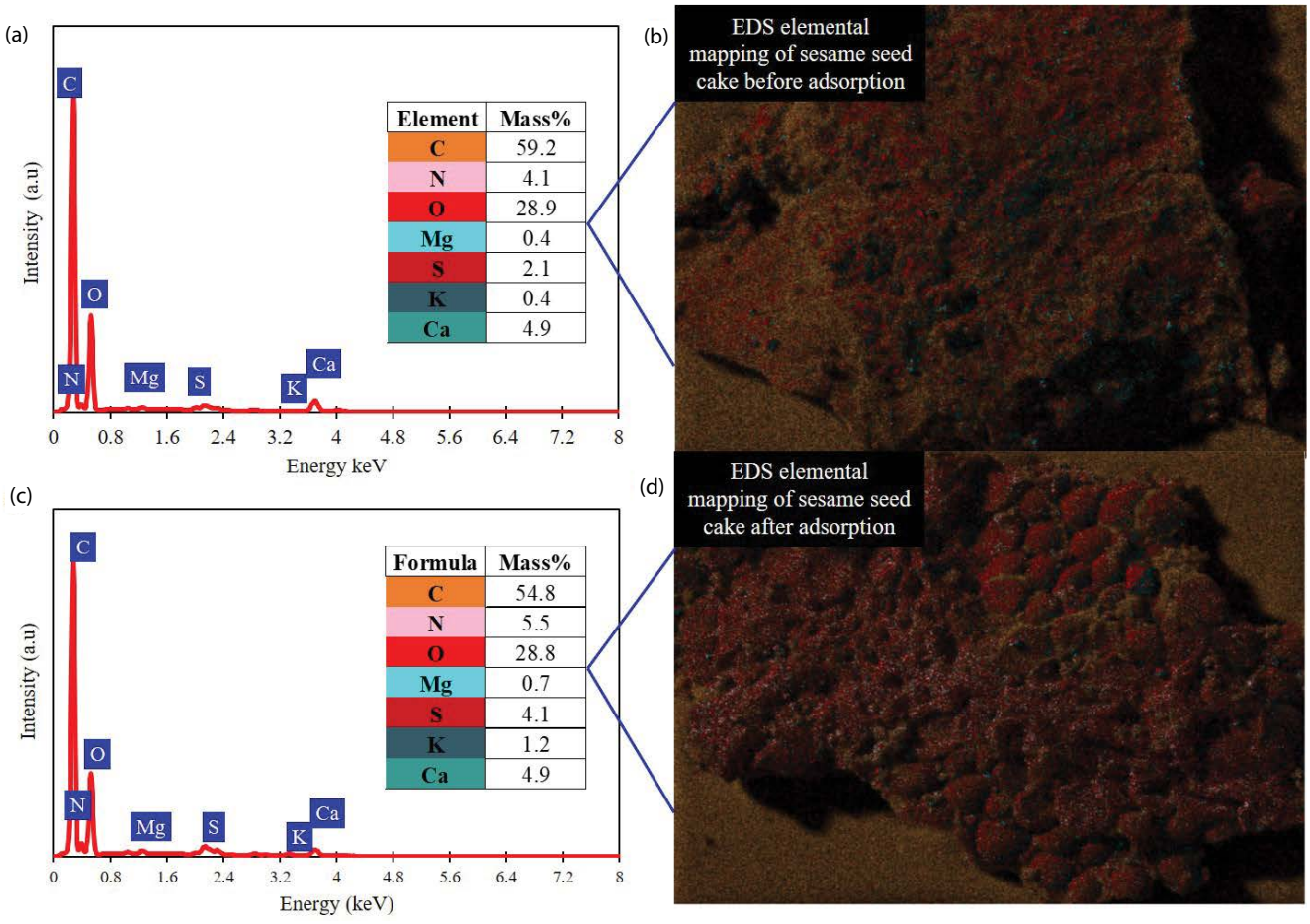

Fig. 2. Elemental composition and mapping of sesame seed cake (a and b) before and (c and d) after adsorption process.

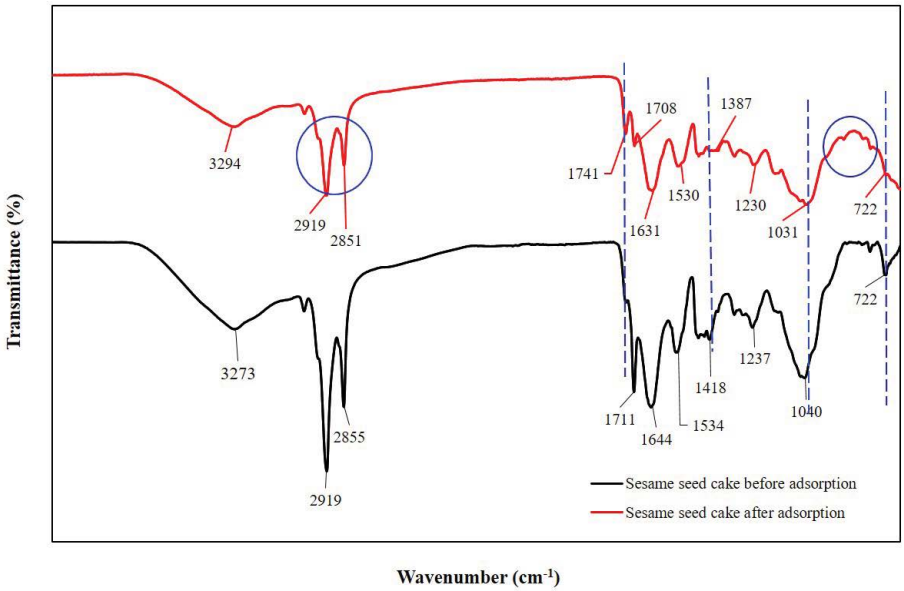

Fig. 3. FTIR spectrum of sesame seed cake before adsorption and after adsorption.

the broad peak observed at 3,273 cm^{-1} was corresponded to OH stretching and vibration, sharp, and narrow peaks seen at 2,919 and 2,855 cm^{-1} were attributed to asymmetric and symmetric vibrations of CH and the stretching vibrations of CH, in methyl and methylene groups, respectively [54]. The peak belongs to OH stretching vibrations exhibited reduced intensity and a shift toward higher wavenumber (3,294 cm^{-1}) after the adsorption of methylene blue. This result revealed that the presence of interaction of dipole–dipole and hydrogen bonding interactions between sesame seed cake and methylene blue [55].

The narrow and strong peak observed at 1,711 cm^{-1} and the medium broad peak appeared at 1,644 cm^{-1} were associated with stretching vibrations of C=O in carboxylate groups and C–N groups in primary amides presence on sesame seed cake [56]. These two peaks slightly shifted and lost their intensities after the adsorption process, because of the possible interaction of these groups with methylene blue dye. Therefore, the narrow and intense peak had just become more visible after the methylene blue adsorption at 1,741 cm^{-1} was attributed to $C{=}N^{+}(CH_3)_2$ stretching vibrations in methylene blue dye [57]. The weak broad peak that appeared at 1,534 cm^{-1} was remarked as skeletal vibrations of C=C bond in the aromatic group [58], and this peak slightly shifted to 1,530 cm^{-1} with decreased intensity mainly attributed with the presence of π–π interactions [55]. The peak observed at 1,418 cm^{-1} was attributed to C–N stretch in amide III. After the adsorption, this peak had almost disappeared due to probably formed electrostatic interactions and a new weak broad peak had become more dominant at 1,387 cm^{-1}. This peak was attributed to symmetrical and asymmetrical bending vibrations of the CH_3 functional groups in methylene blue dye. The weak peak observed at 1,237 cm^{-1} was attributed to heterocycle vibrations of C–C [57] and this peak slightly shifted to 1,230 cm^{-1} after the adsorption process. The broad strong peak observed at 1,040 cm^{-1} was attributed to angular deformation of C–O groups [56] in sesame seed cake and this peak slightly shifted and had become more broad appeared at 1,031 cm^{-1}. This significant decrease in the intensity of the C–O peak after the adsorption mainly indicated that *n*–π interactions played a role in the adsorption process [55]. In this interaction, the oxygen groups on the sesame seed cake acted as electron donors and while the aromatic rings of methylene blue dye acted as electron acceptors [59]. Therefore, after the adsorption of methylene blue dye on sesame seed cake, two small peaks appeared at 882 and 761 cm^{-1}. These two peaks were attributed to the presence of C–H out of plane deformation and C–Cl stretch, respectively in methylene blue. Finally, the last weak and medium peak observed at 722 cm^{-1} resulted from CH out of plane deformation in CH=CH groups present in alkenes [60,61]. This peak had almost disappeared after the adsorption process due to the possible interaction of these groups with methylene blue dye. Thus, it was concluded that methylene blue was adsorbed on sesame seed cake as a consequence of some physical interactions characterized by the strong presence of OH^{-} groups since the related peaks slightly shifted and lost the first intensities. In addition, another conclusion was revealed from the FTIR results that the chemical interactions characterized by electrostatic interactions also involved in the adsorption of methylene blue dye on sesame seed cake due to the disappearance of some peaks.

As FTIR and SEM revealed the proposed complex interaction mechanism between the sesame seed cake and methylene blue is illustrated in Fig. 4 by using recent studies [59,62,63]. In this schematic view of the proposed interaction mechanism, the backbone of the sesame seed cake was illustrated as a carbon-based backbone as confirmed in EDX analysis. The possible functional groups at the surface of the sesame seed cake were located as found in FTIR analysis.

BET analysis was also applied on sesame seed cake before and after the methylene blue adsorption. The nitrogen (N_2) adsorption–desorption isotherms and pore size

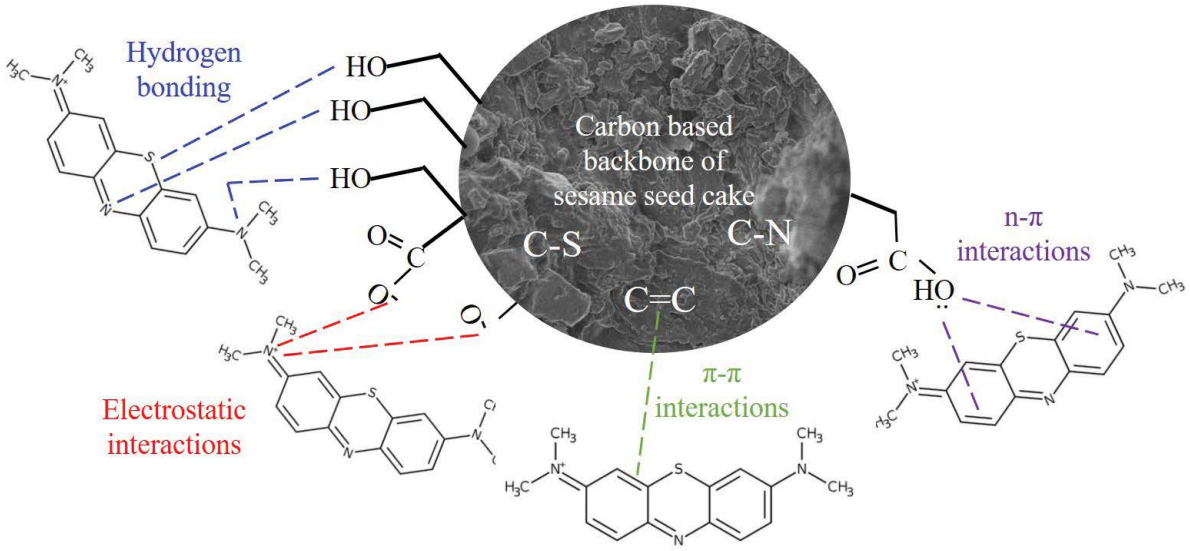

Fig. 4. Proposed interaction mechanism between methylene blue and sesame seed cake.

distribution of the sesame seed cake before and after the adsorption are given in Figs. 5a–d. The total pore volume was estimated to be the liquid volume of N_2 at a relative pressure of 0.99. Because, at this point, all the pores of the samples were already filled with N_2 [22]. According to the obtained results, the N_2 adsorption–desorption isotherms of sesame seed cake before and after the adsorption showed that the isotherms exhibited type IV with H3 hysteresis structure which is characterized by mesoporous materials classified by IUPAC classification [64]. Before the adsorption process, BET surface area and total pore volume of the sesame seed cake were found as 0.1257 ± 0.0276 m^2/g and 0.00091 cm^3/g, respectively, while after the adsorption process they were found as 0.0277 ± 0.0019 m^2/g and 0.00125 cm^3/g, respectively. The significant reduction in surface area of the sesame seed cake [21,65] proved that the methylene blue mostly penetrated on the surface of the sesame seed cake causing the blockage of some pores. Besides, a slight increase in the total pore volume of the sesame seed was attributed to the possible interaction between the neighborhood pores.

As can be seen in Figs. 5b and d, the pore size distribution changed after the methylene blue adsorption. However, since the total pore volume of the sesame seed cake was not changed significantly, it could be deduced that the methylene blue mostly penetrated on the surface of the sesame seed cake rather than the inside of the pores. Generally, almost all low-cost bio-waste agricultural adsorbents without any pretreatment are characterized by low surface area. Hence, the high methylene blue adsorption on sesame seed cake such a having low surface area was directly attributed to some strong interactions playing an important role in the adsorption process [66]. As explained previously, the interactions classified as electrostatic, n–π and π–π interactions and hydrogen bonding had played a significant role in the adsorption process.

In Fig. 6, the variation of pH difference (ΔpH) between the initial pH value (pH_i) and final pH value (pH_f) vs. the pH_i values is given. According to Fig. 6, the pH_{PZC} value of sesame seed cake was found at about 6.5 and this result represents that the surface of the adsorbent has net-zero surface charge at this point. On the other hand, the surface of the sesame seed cake had positively charged at pH values below of pH_{PZC} value whereas the sesame seed cake has negatively charged at pH values above pH_{PZC} [67]. Therefore, this result revealed that the sesame seed cake surface could be used for the removal of different categories of dyes since the surface of the sesame seed cake could be switched according to the pH of the aqueous solution.

3.2. Optimization studies on methylene blue removal

In the present study, temperature (A), pH (B), and adsorbent dosage (C) were considered as independent process variables, and the removal percentage of methylene blue was considered as a response. The optimum conditions of the methylene blue removal were assessed using BBD coupled with RSM. The list of experiments designed by RSM and the values of response for each sample obtained at corresponding experimental conditions are represented in Table 2. According to the results obtained, the maximum and minimum methylene blue dye removal percentage was found as 94.18 (at the temperature of 30°C, pH of 9 and 3 g/100 mL adsorbent dosage) and 62.0 (at the temperature of 30°C, pH of 3 and 1 g/100 mL adsorbent dosage), respectively.

The optimum conditions for high methylene blue dye removal were determined by taking into consideration of lower energy and minimum adsorbent dosage requirements. Thus, the optimum condition of methylene blue dye on sesame seed cake was determined at the point including the temperature of 20°C, pH of 9, and adsorbent dosage of 2 g/100 mL. Later on, the regression analysis was performed to be clear about the relationship between the independent process variables and response. The final equation fitting to the quadratic model was suggested by the BBD method and

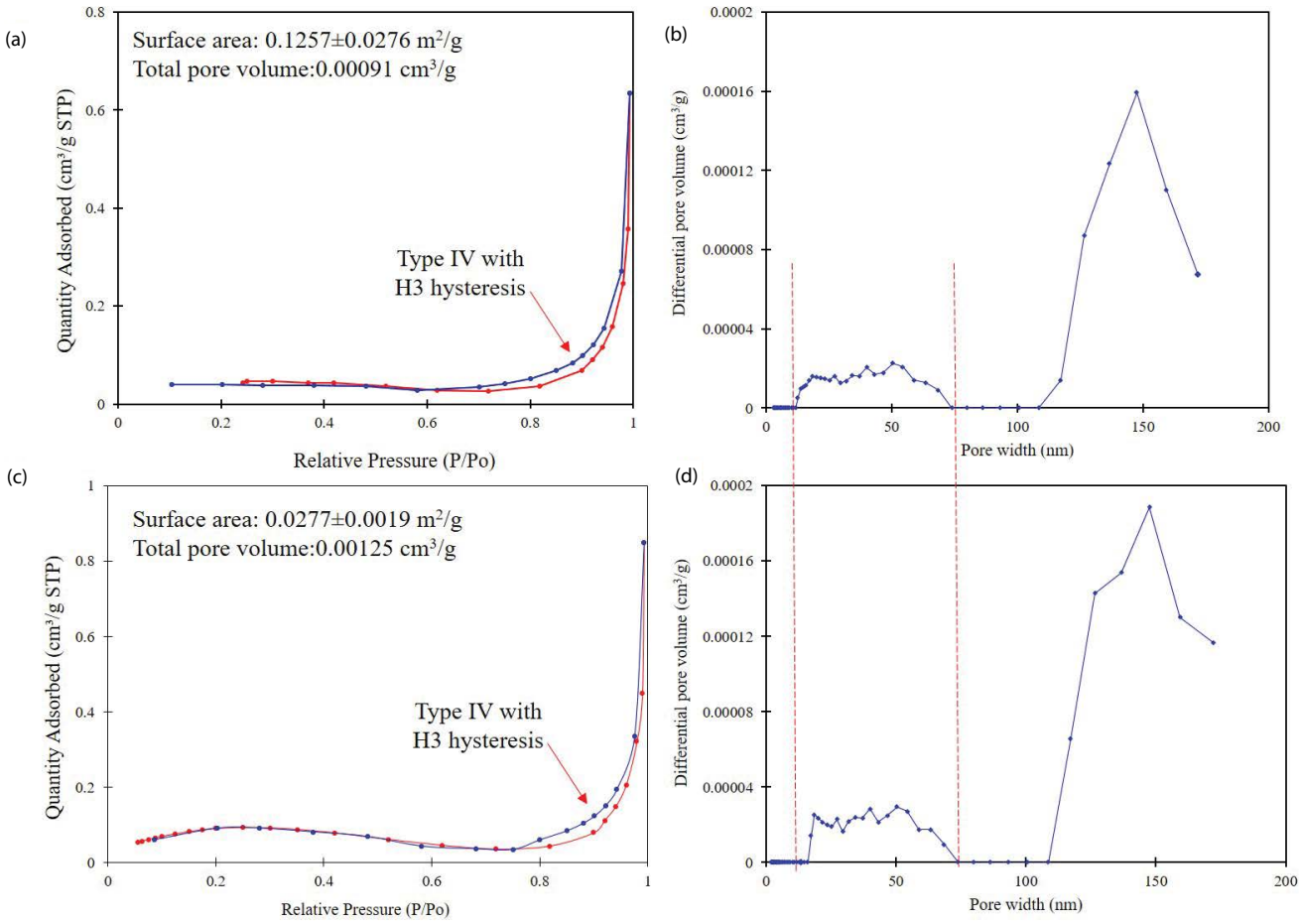

Fig. 5. N_2 adsorption–desorption isotherms pore size distribution of sesame seed cake before (a and b, respectively) and after adsorption (c and d, respectively).

the equation was expressed in terms of the coded factors as following:

$$R_1 = 16.505 + 0.278A + 11.163B + 13.703C - 0.017AB + 0.023AC - 0.567BC - 0.002A^2 - 0.480B^2 - 1.490C^2 \quad (4)$$

The ANOVA was carried out to determine the adequacy of the developed model and the significance of the suggested constant coefficients. Additionally, this analysis explored that the individual, interactive, and quadratic effects of the independent process variables on the removal of methylene blue using sesame seed cake. The data obtained from ANOVA analysis are represented in Table 3.

The individual, interactive, and quadratic significance of the independent process variables were evaluated using their *p*-values determined by ANOVA analysis. The *p*-value less than 0.05 indicates that the model term is statistically important and should be used in the model equation. In the present study, *A*, *B*, *C*, *BC*, B^2, and C^2 were found as significant model terms. Besides, the ANOVA analysis is also a guide to determine the most affecting term on the methylene blue removal from aqueous solutions and the *F*-values of each term are used [3]. The most affecting terms were ordered as: $B > C > B^2 > BC > C^2 > A > AB > AC > A^2$.

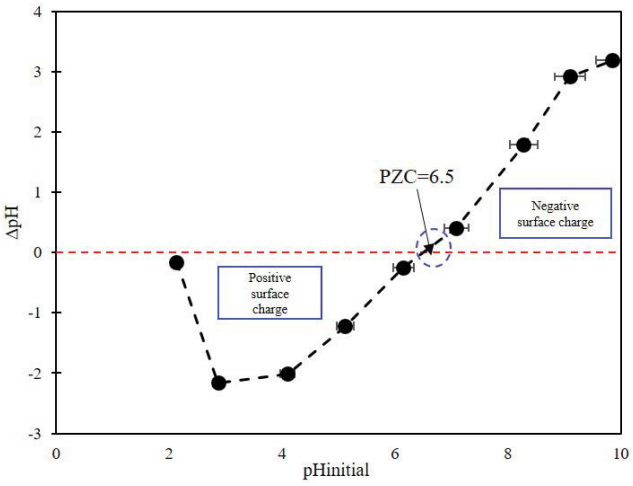

Fig. 6. Point of zero charge determination of sesame seed cake.

According to this finding, the most affecting parameter on methylene blue removal was found as pH which is a parameter that controls the magnitude of electrostatic charges of the medium. The percentage of the methylene blue removal

Table 2
Experimental design and response values for methylene blue adsorption

Run	Independent process variables						Response
	Temperature (°C)		pH		Adsorbent dosage (g/100 mL)		Removal rate of methylene blue (%)
	Uncoded	Coded	Uncoded	Coded	Uncoded	Coded	
1	30	(0)	3	(–1)	3	(1)	74.91
2	20	(–1)	6	(0)	3	(1)	87.62
3	30	(0)	6	(0)	2	(0)	85.97
4	20	(–1)	6	(0)	1	(–1)	77.47
5	30	(0)	6	(0)	2	(0)	85.04
6	30	(0)	9	(1)	1	(–1)	88.07
7	20	(–1)	9	(1)	2	(0)	92.26
8	30	(0)	6	(0)	2	(0)	85.82
9	30	(0)	3	(–1)	1	(–1)	62.00
10	30	(0)	6	(0)	2	(0)	85.79
11	40	(1)	6	(0)	1	(–1)	79.72
12	20	(–1)	3	(–1)	2	(0)	68.79
13	40	(1)	3	(–1)	2	(0)	70.91
14	30	(0)	6	(0)	2	(0)	85.36
15	30	(0)	9	(1)	3	(1)	94.18
16	40	(1)	6	(0)	3	(1)	90.78
17	40	(1)	9	(1)	2	(0)	92.32

Table 3
ANOVA analysis data for the developed Quadratic model

Source	Sum of squares	df	Mean square	*F*-value	*p*-value	Significance
Model	1,331.89	9	147.99	410.65	<0.0001	Significant
A: Temperature	7.20	1	7.20	19.98	0.0029	
B: pH	1,017.46	1	1,017.46	2,823.36	<0.0001	
C: Adsorbent dosage	202.31	1	202.31	561.38	<0.0001	
AB	1.06	1	1.06	2.94	0.1299	
AC	0.2070	1	0.2070	0.5745	0.4732	
BC	11.56	1	11.56	32.08	0.0008	
A^2	0.1844	1	0.1844	0.5116	0.4976	
B^2	78.46	1	78.46	217.72	<0.0001	
C^2	9.34	1	9.34	25.91	0.0014	
Residual	2.52	7	0.3604			
Lack of fit	1.93	3	0.6434	4.34	0.0950	Not significant
Pure error	0.5925	4	0.1481			
Cor. total	1,334.41	16				

will increase at a high pH value as expected since the methylene blue dye is a cationic dye. The underlying reason for this case could be explained as increasing the negatively charged surface sites on adsorbent at high pH value and thus, stronger interaction between the adsorbent and methylene blue dye molecules [13]. The results obtained to support this mechanism, and the removal percentage of the methylene blue was increased at a higher pH value. The comparison of the individual effects of independent process variables was also assessed by the perturbation plot (Fig. 7). The sharp curvature of pH (*B*) also supported that the pH value was the most affecting independent process variable for methylene blue removal [68].

According to the ANOVA analysis, Fisher's *F*-value of the model was found as large as to indicate that the suggested quadratic model was significant. The ANOVA data also reveals that there is only a 0.01% chance that model *F*-value this large could occur due to noise. Additionally, there is a 9.50% chance that a lack of fit *F*-value this large could occur due to noise, and this value should be non-significant to fit

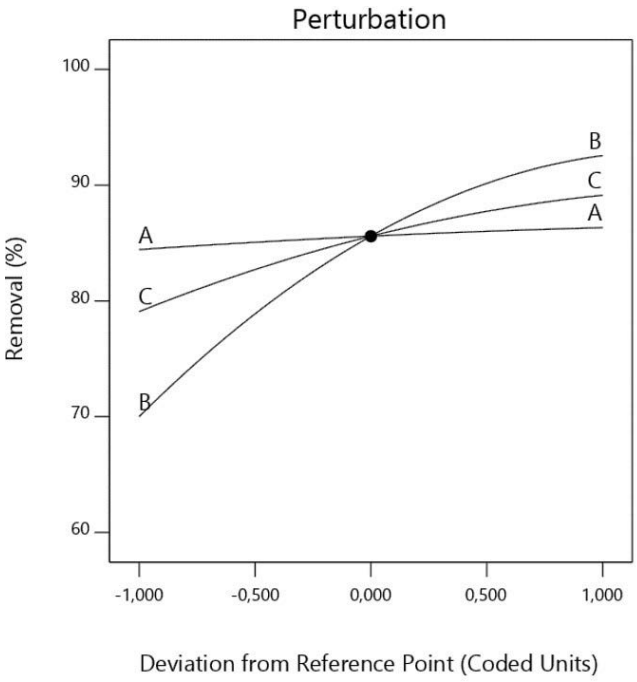

Fig. 7. Perturbation plot of methylene blue adsorption onto sesame seed cake with coded terms.

the suggested model to the experimental data. Thus, these two meaningful approaches to understanding whether the suggested model is significant or not indicated the statistical significance of the suggested model.

The model summary statistic was suggested by the developed quadratic model as can be seen in Table 4. The reasonable agreement within the predicted correlation of coefficient (R^2 = 0.9762) and adjusted correlation of coefficient (R^2 = 0.9957) values, confirmed a high correlation between the predicted and experimental results. The statistical parameters and the actual and predicted responses

Table 4
Statistical parameter values

Statistical parameters	Values
R^2	0.9981
Adjusted R^2	0.9957
Predicted R^2	0.9762
Adequate precision	70.8327

of methylene blue removal are given in Fig. 8a. The actual values were representing the experimentally obtained values, and the predicted values were representing the model response. The adequate precision measures signal to noise ratio and the value of adequate precision greater than 4 is desirable. In the present study, the adequate precision ratio was found as 70.8327 (Table 4). It means that the developed quadratic model could be used to express the methylene blue removal by using sesame seed cake.

The insignificant terms could be removed from the developed quadratic model for the accurate prediction of the response if the actual and predicted response results did not fit each other. In the present study, this situation was deeply examined, and it was concluded that the removal of any of the terms was not essential because the actual and predicted response obtained had a reasonable agreement, and also no significant abnormal distribution of the error terms were found. The normal probability plots of the residuals are represented in Fig. 8b. The linear relationship between the internally studentized residuals and normal % probability was the expected result to conclude that the error terms were indeed normally distributed with minimum deviations, hence there was not any required transformation on the developed quadratic model given in Eq. (4) [3,69,70].

The conjugated effect of temperature and pH, temperature and adsorbent dosage, pH, and adsorbent dosage was assessed by using two independent process variables

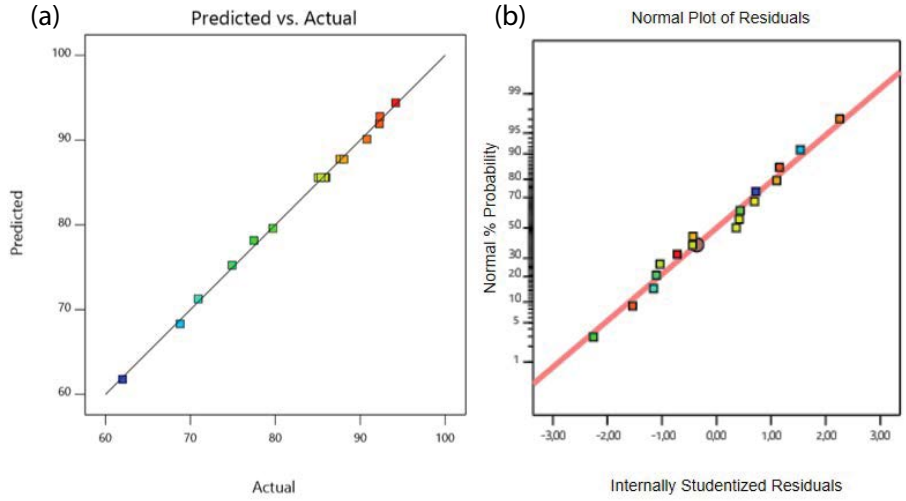

Fig. 8. (a) Predicted data vs. actual data of methylene blue removal percentage and (b) normal plots of residuals for methylene blue adsorption on sesame seed cake.

while keeping the other process variables at the central (0) level. The corresponding two-dimensional (2D) contour plots and three-dimensional (3D) response surface plots are given in Figs. 9a–c. In Fig. 9a, the combined effect of temperature and pH for methylene blue removal at the constant adsorbent dosage and initial concentration of methylene blue is depicted. As can be seen in Fig. 9a, the increase of pH value provided efficient methylene blue

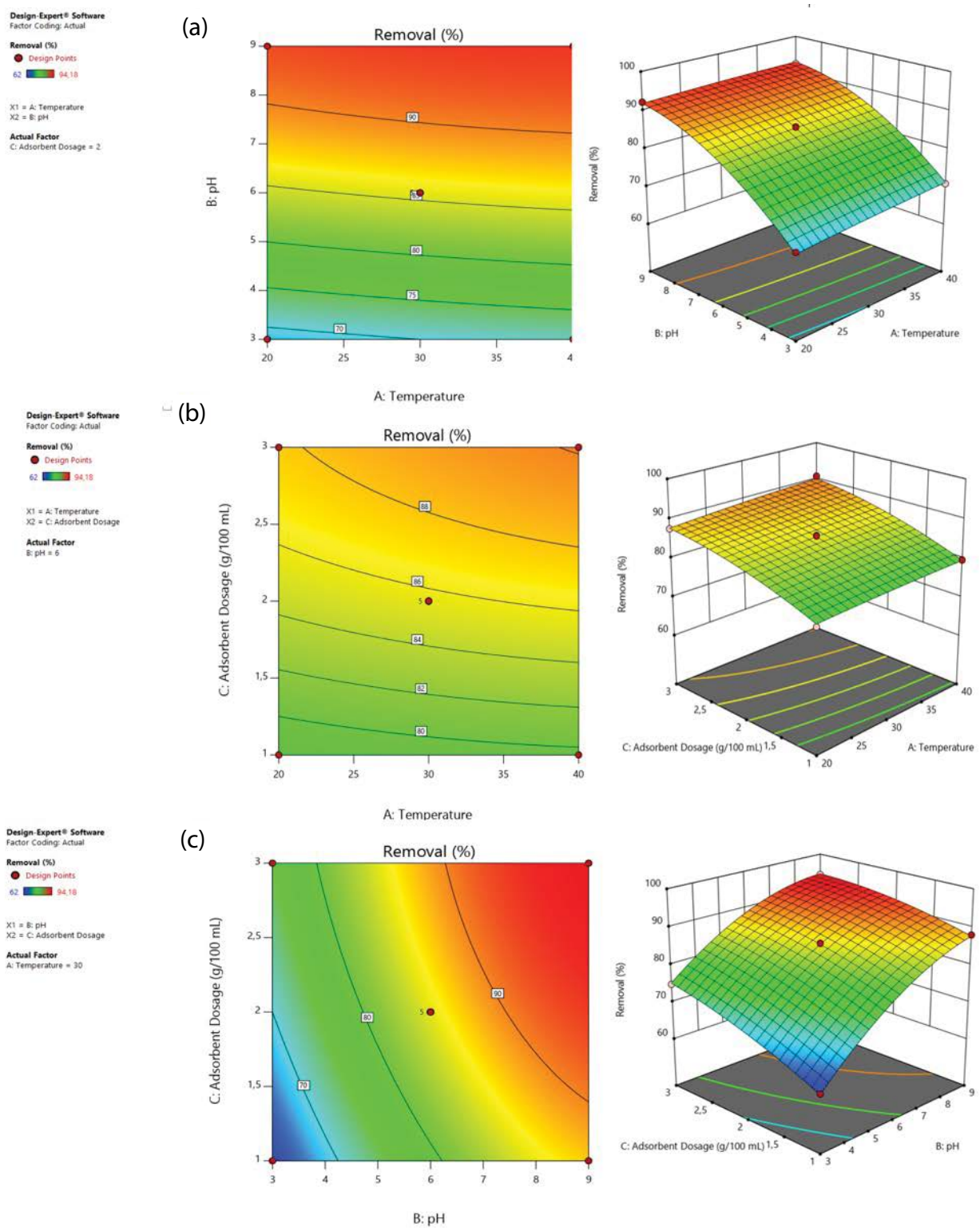

Fig. 9. 2D and 3D surface plots of the effect of (a) temperature and pH at constant adsorbent dosage, (b) temperature and adsorbent dosage at constant pH, (c) pH and adsorbent dosage at the constant temperature for methylene blue removal onto sesame seed cake.

removal. However, at constant pH value, the increase of temperature did not seem to be a highly effective independent parameter when compared with the other parameters.

In Fig. 9b, 2D and 3D surface plots of the effect of temperature and adsorbent dosage at constant pH for methylene blue removal onto sesame seed cake are given. The color change from green to light orange in Fig. 9b indicates that the combined effect of temperature and adsorbent dosage slightly changed the methylene blue removal. The same result had been also revealed by assessing *F*-values of the variables and the combined effect of temperature and adsorbent dosage (*AC*) had been also found as almost the lowest affecting parameter on methylene blue removal.

The combined effect of pH and adsorbent dosage (*BC*) had been found as the most effective parameter among other combined effects of independent process variables (*AB* and *AC*) because it had the highest *F*-value. In Fig. 9c, this result was also confirmed by sharp curvature and color changing of the plot. It was noticed that the high pH and adsorbent dosage values provide high methylene blue removal. Additionally, at constant pH values, change in adsorbent dosage had a more significant effect on methylene blue removal when it was compared with temperature (Fig. 9c).

3.3. Adsorption kinetic studies on methylene blue removal

The adsorption kinetic studies describe the rate of retention or release of adsorbent from aqueous solutions to a solid-phase interface at a specified temperature, pH, and adsorbent dosage. The kinetic studies are mostly applied to predict the rate of the removal of the contaminant from the aqueous solution to design an adsorption treatment plant. The adsorption kinetic studies enlighten the controlling step and mechanism of the adsorption. The kinetic studies of methylene blue adsorption were conducted with 200 ppm initial concentration of methylene blue solution at optimum condition (temperature of 20°C, pH of 9, and adsorbent dosage of 2 g/100 mL) by withdrawing samples at determined time intervals. Then, the methylene blue removal was determined by UV-spectrophotometer at 664 nm wavelength. The effect of contact time on methylene blue removal (%) is given in Fig. 10a at the mentioned optimum condition. It can be seen that the methylene blue adsorption had rapidly increased in 5 min and achieved equilibrium within almost 20 min. The fast initial removal of methylene blue dye on sesame seed cake could be attributed to the formation of strong hydrogen bonds between the methylene blue and sesame seed cake as indicated by the FTIR spectrum [71]. The UV-vis absorption spectra of aqueous methylene blue solution before and after the adsorption process were recorded in a range from 800 to 400 nm with a 0.5 nm data interval. The results are given in Fig. 10b. According to the results obtained, the downward trend in intensity of two characteristic absorbance shoulders of methylene blue without any significant shift of the wavelength was observed. This result directly indicated that the methylene blue adsorption was the sole process taking place on sesame seed cake.

In the present study; pseudo-first-order, pseudo-second-order, and Elovich kinetic models were separately

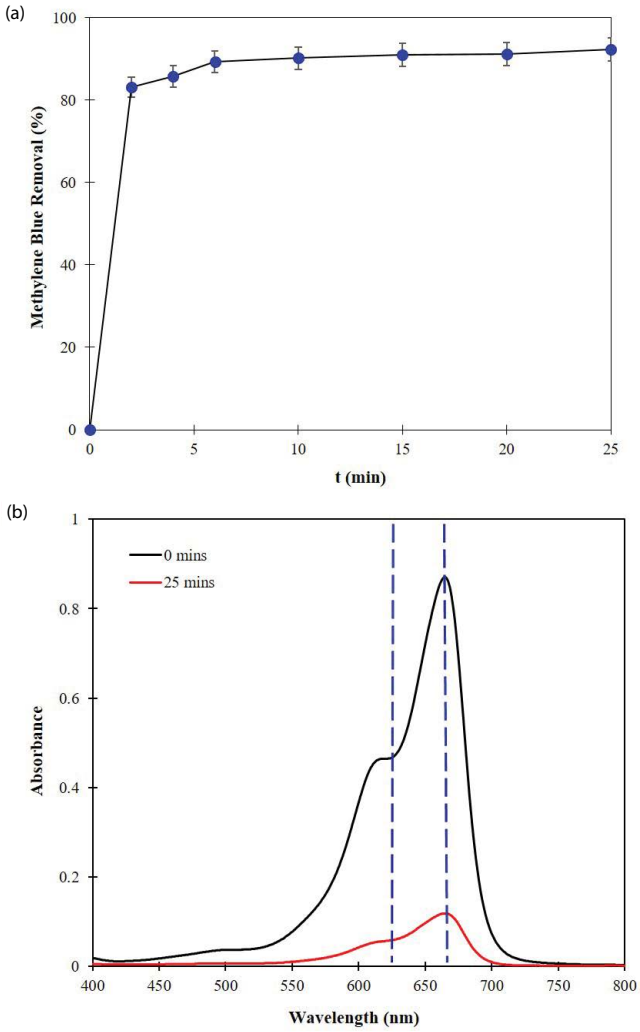

Fig. 10. (a) Effect of contact time on methylene blue removal (%) for optimum conditions of temperature 20°C, pH 9, and adsorbent dosage 2 g/100 mL and (b) UV-vis spectra of aqueous methylene blue solution before and after the adsorption.

applied for the determination of the best-fitted model with the experimental results. These kinetic model equations in linearized forms and parameters are given in Table 5.

The experimental data related to the methylene blue removal (%) were used to calculate the experimental q_e and q_t parameters. The linear equations which are specific for each kinetic model as presented in Table 5 were used to set the linear plots and to investigate the appropriate kinetic model, which is the best fit with the methylene blue adsorption experimental data. The values of kinetic model parameters, correlation coefficients (R^2), and standard deviation (σ) for each kinetic model are given in Table 6.

The pseudo-first-order model which is the earliest model suggested by Lagergren describes the adsorption rate based on the adsorption capacity [19]. This model is mainly characterized by diffusion through a boundary [13]. Otherwise the pseudo-second-order kinetic model dependent on the amount of solute adsorbed on the adsorbent surface and the adsorbed amount at equilibrium

Table 5
Kinetic model equations applied in the present study

Models	Linearized equations	Parameters
Pseudo-first-order kinetic [21]	$\ln(q_e - q_t) = \ln q_e - k_1 t$	q_e = adsorption capacity (mg/g) at equilibrium q_t = adsorption capacity (mg/g) at any time k_1 = equilibrium rate constant (1/min) of pseudo-first-order kinetic model
Pseudo-second-order kinetic [21]	$\frac{t}{q_t} = \frac{1}{q_e^2 k_2} + \frac{t}{q_e}$	q_e = adsorption capacity (mg/g) at equilibrium q_t = adsorption capacity (mg/g) at any time k_2 = equilibrium rate constant (g/mg min) of pseudo-second-order kinetic model
Elovich kinetic [66]	$q_t = \frac{1}{\beta}\ln(\alpha\beta) + \frac{1}{\beta}\ln t$	α = initial sorption rate constant (mg/g min) β = Elovich constant (desorption constant)

Table 6
Kinetic model parameters of the methylene blue removal by sesame seed cake

Models	Kinetic model parameters				
Pseudo-first-order kinetic model equation	$q_{e,\text{experimental}}$ (mg/g)	$q_{e,\text{predicted}}$ (mg/g)	k_1 (1/min)	R^2	σ
$\ln(q_e - q_t) = -0.2312t + 1.2115$	9.1979	3.3585	0.2312	0.8116	0.8204
Pseudo-second-order kinetic model equation	$q_{e,\text{experimental}}$ (mg/g)	$q_{e,\text{predicted}}$ (mg/g)	k_2 (g/mg min)	R^2	σ
$t/q_t = 0.1071t + 0.0519$	9.1979	9.3371	0.2210	0.9995	0.0203
Elovich kinetic model equation	–	α (mg/g min)	β (g/mg)	R^2	σ
$q_t = 0.3518 \ln t + 8.0025$	–	26.6273	2.8425	0.8716	0.1374

[72]. This model assumed that the rate-controlling step might be the chemisorption [13]. On the other hand, several studies are revealing that the physical and chemical interactions could not be strictly distinguishable if there are both physical and chemical interactions involved in the adsorption process especially in presence of strong hydrogen bonds [73,74]. The kinetic studies revealed that the pseudo-second-order kinetic model was the best appropriate model representing the methylene blue adsorption kinetics by sesame seed cake due to the highest value of R^2 = 0.9995 and the lowest standard deviation (σ = 0.0203) among other kinetic models examined. As can be seen in Table 6, the calculated q_e values have a good agreement with the experimental q_e values, and this finding reconfirms the applicability of the pseudo-second-order kinetic model. The linearized pseudo-second-order kinetic model plot is given in Fig. 11.

Besides, the parameters of the Elovich kinetic model indicate a high affinity between methylene blue molecules with sesame seed cake since the β (desorption constant) value was found highly lesser than the α value (initial sorption rate) [75].

Since the high correlation of coefficient value and low standard deviation obtained from the pseudo-second-order kinetic model, it was impossible to understand which specific adsorption step was significant for the methylene blue adsorption on sesame seed cake. When the adsorbent material contact with a solution including dye molecules, there are three main steps observed during the adsorption process of dye molecules on the adsorbent material.

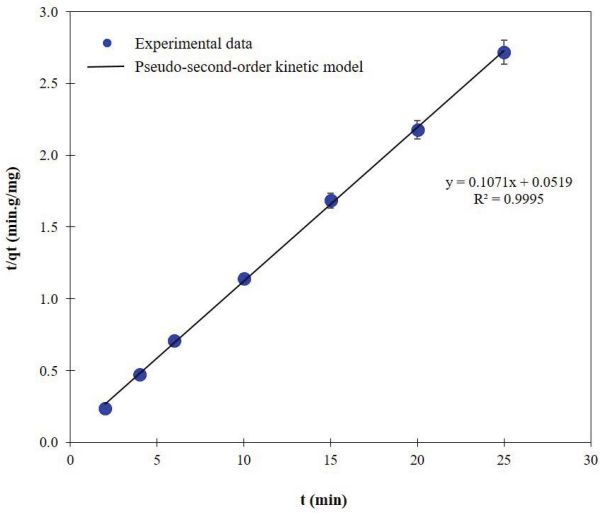

Fig. 11. Plot of a pseudo-second-order kinetic model for methylene blue adsorption on sesame seed cake.

The first step is associated with the migration of dye molecules from the bulk solution to the surface of the liquid film, thus, to the external surface of the adsorbent, and this step is also called film diffusion. The penetration of dye molecules to the pores of the adsorbent (intra-particle diffusion) is the second step. In the final step; adsorption and desorption take place on the interior surface of the adsorbent are observed [76–78]. The total adsorption rate

is characterized by either the first step or second step or both of them since the third step is considered to be as fast as could not be a rate-liming step [78]. In the present study, the adsorption mechanism of methylene blue on sesame seed cake was deeply investigated by applying to additive kinetic models called intra-particle diffusion kinetic model and Boyd plot analysis (Table 7), and the contribution of the mentioned three steps was understood.

The intra-particle diffusion kinetic model is introduced to describe the contribution of intra-particle diffusion to the sorption mechanism since the pseudo-first-order and pseudo-second-order kinetic models do not elucidate the diffusion mechanism of adsorbate on adsorbents [27,72]. According to the literature, the plot of q_t vs. $t^{1/2}$ should give a straight line with passing through the origin if the intra-particle diffusion is the sole rate-limiting step [27,79]. In the present study, the plot of q_t vs. $t^{1/2}$ comprised of two linear parts as shown in Fig. 12a. Even though the plot was not associated with the straight line passing through the origin, it gave an insight into the possible stages that occurred during the methylene blue adsorption on sesame seed cake. According to the literature, the multilinear character of the plot confirmed that the adsorption of methylene blue on sesame seed cake had a multistage of adsorption [8]. In this case, k_{id} values are calculated from the slope of each linear part. In the present study, k_{id} value of the first linear part (k_{id1}) and final part (k_{id2}) were found as 5.88 (mg/g min$^{1/2}$) and 0.228 (mg/g min$^{1/2}$), respectively (Table 8). As could be seen, the first k_{id} value was found as larger than the second k_{id} value and this situation was attributed to a higher adsorption rate in the first part related to the availability of the adsorption sites at the initial part [76]. The first linear part observed at 0–2 min was attributed to external surface adsorption characterized by boundary layer diffusion taking place at larger pores

Table 8
Parameters of intra-particle diffusion

Intra-particle diffusion model parameters			
k_{id1} (mg/g min$^{1/2}$)	R^2	k_{id2} (mg/g min$^{1/2}$)	R^2
5.88	1	0.228	0.91

Table 7
Intra-particle diffusion kinetic model and Boyd plot kinetic model equations

Kinetic models	Kinetic model equations	Parameters
Intra-particle diffusion kinetic model [21]	$q_t = k_{id}t^{1/2} + C_i$	k_{id} = intra-particle diffusion rate constant (mg/g min$^{1/2}$) C_i = constant (mg/g)
Boyd plot kinetic model [27]	$B_t = -0.4977 - \ln\left(1 - F(t)\right)\ \ F(t) > 0.85$ $B_t = \left[\sqrt{\pi} - \sqrt{\left(\pi - \left(\frac{\pi^2 - F(t)}{3}\right)\right)}\right]^2\ \ F(t) > 0.85$	$F(t)$ = fractional attainment of equilibrium at different times (q_t/q_e)

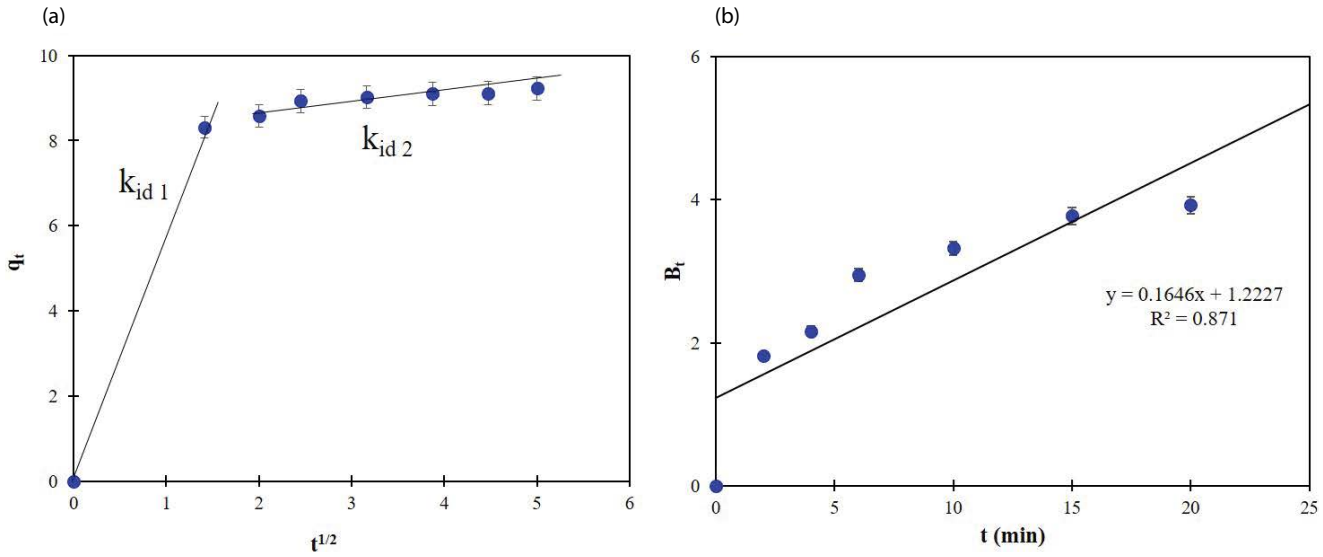

Fig. 12. (a) Plot of $t^{1/2}$ vs. q_t and (b) Boyd plot.

[76]. The final linear part of the plot was characterized by intra-particle diffusion in which the adsorption mainly took place at the interior of the pores [27]. This result indicated that the adsorption was not only controlled by the intra-particle diffusion, there was also film diffusion contribution [80].

As the intra-particle diffusion was not found as a sole rate-limiting step, the Boyd plot analysis was applied to investigate the contribution of film resistance to the kinetics of methylene blue adsorption on sesame seed cake. If the plot of B_t vs. t gives a straight line passing through the origin, it implies that the actual rate-limiting step is intra-particle diffusion [81]. Otherwise, as observed in the present study, the rate-limiting step is determined as the film diffusion or chemical reaction [71]. The plot of B_t vs. t was plotted with a 0.871 correlation coefficient (R^2) (Fig. 12b). As can be seen from Fig. 12b, since the plot was not passing through the origin, the possible dominant mechanism of methylene blue adsorption on sesame seed cake was determined as film diffusion or chemical reaction.

3.4. Adsorption isotherm studies on methylene blue removal

The adsorption isotherm modeling studies were conducted to indicate the adsorbate interaction with the adsorbent and the adsorption capacity of the adsorbent. Additionally, the distribution of adsorbent particles between the liquid phase and the solid phase at the equilibrium point of the adsorption process [82]. Besides, the adsorption isotherm models indicate the distribution of adsorbents. Hence, the adsorption isotherm studies were performed at optimum temperature and pH conditions (temperature of 20°C and pH of 9) at various adsorbent dosages from 0.5 to 4 g/100 mL. The experimental data obtained from the adsorption isotherm studies were used to fit with the adsorption isotherm models such as Langmuir, Freundlich, Temkin, and Dubinin–Radushkevich. The linearized forms of those isotherm models are given in Table 9.

Langmuir isotherm model is representing the monolayer adsorption and the R_L value called a separation factor gives information if the adsorption process is favorable ($0 < R_L < 1$), unfavorable ($R_L > 1$), linear ($R_L = 1$), or irreversible ($R_L = 0$) [3,16]. In the present study, even if the relatively low correlation of coefficient value ($R^2 = 0.9301$) blocked the usage of this model to describe the methylene blue adsorption on sesame seed cake, the R_L value was calculated to get an insight into whether the adsorption is favorable or not. The R_L value was found as 0.45 which means that the methylene blue adsorption on sesame seed cake was favorable. According to the obtained data from the adsorption isotherm studies, the adsorption isotherm model parameters were calculated and are represented in Table 10.

Freundlich isotherm model based on the heterogeneous adsorption surface having unequal available sites with various adsorption energies and various affinities [22,16]. The linear fitting of Freundlich isotherm model was displayed in Fig. 13 to determine the nature of the interaction between methylene blue and sesame seed cake at equilibrium.

According to Fig. 13 and Table 10, the highest correlation of coefficient ($R^2 = 0.9986$), lowest standard deviation ($\sigma = 0.0419$), and best linear line were found for Freundlich adsorption isotherm model. Thus, it was concluded that the Freundlich isotherm model was found to be the best model describing the methylene blue adsorption on sesame seed cake. Generally, n value bigger than 1 indicates that the adsorbate is favorably adsorbed on the adsorbent whereas the n value smaller than 1 points out that the chemical adsorption process in nature [8,22,49]. In the present study, the n value was found as 1.2679 and it indicated that the methylene blue was adsorbed on sesame seed cake, favorably and controlled by order of physical adsorption [8,22,49,83,84]. In addition, the n value in the range of 1–10

Table 9
Linearized forms of adsorption isotherm models

Models	Linearized equations	Parameters
Langmuir isotherm model [83]	$\frac{C_e}{q_e} = \frac{C_e}{q_m} + \frac{1}{K_a \times q_m}$	q_e = adsorption capacity (mg/g) at equilibrium q_m = maximum adsorption capacity (mg/g) K_a = Langmuir constant (L/mg) C_0 = initial concentration (ppm) of methylene blue $R_L = 1/(1 + K_a C_0)$
Freundlich isotherm model [83]	$\ln q_e = \ln K_f + \left(\frac{1}{n}\right) \ln C_e$	q_e = adsorption capacity (mg/g) at equilibrium C_e = methylene blue concentration at equilibrium (mg/L) K_f = Freundlich equilibrium constant ((mg/g))/(L/mg)$^{1/n}$ n = empirical constant
Temkin isotherm model [66]	$q_e = B \ln A_t + B \ln C_e$	$B = RT/b$, R = gas constant b = heat of adsorption constant (J/mol) A_t = Temkin equilibrium binding constant (L/g)
Dubinin–Radushkevich isotherm model [84]	$\ln q_e = \ln q_m - \beta \varepsilon^2$	q_e = adsorption capacity (mg/g) at equilibrium q_m = maximum adsorption capacity (mg/g) $\varepsilon = RT \ln(1 + (1/C_e))$, R = gas constant β = constant related with adsorption free energy (mol^2/kJ^2)

Table 10
Adsorption isotherm model parameters

Models	Kinetic model parameters			
Langmuir isotherm model equation	q_m (mg/g)	K_a (L/mg)	R^2	σ
$C_e/q_e = 0.0092C_e + 1.5289$	108.69	0.006	0.9301	0.5956
Freundlich isotherm model equation	n	K_f (L/mg)	R^2	σ
$\ln q_e = 0.7887 \ln C_e + 0.0544$	1.2679	1.0559	0.9986	0.0419
Temkin isotherm model equation	A_t (L/g)	b (J/mol)	R^2	σ
$q_e = 10.439 \ln C_e - 17.36$	0.1895	244.60	0.9264	3.0433
Dubinin–Radushkevich isotherm model equation	q_m (mg/g)	β (mol²/kJ²)	R^2	σ
$\ln q_e = 2.8707 - 12.784\varepsilon^2$	17.64	12.784	0.85	0.42

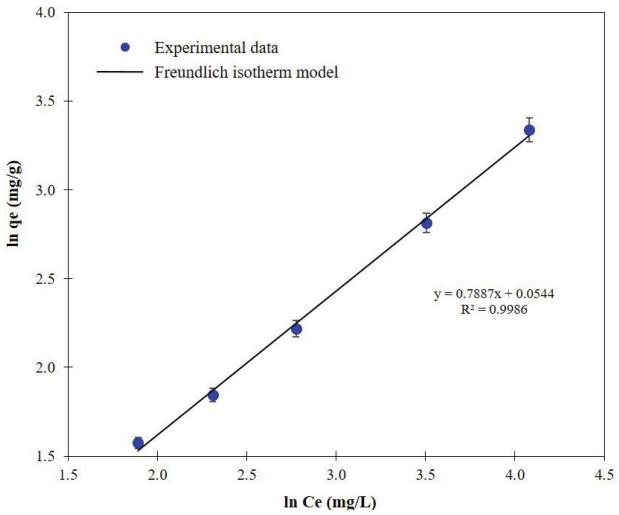

Fig. 13. Plot of the Freundlich isotherm model for methylene blue adsorption on sesame seed cake.

represents good adsorption with a reasonable surface density [83]. Here in, even if the found n value is in the field of physical adsorption energy, the adsorption of methylene blue on sesame seed cake could be explained by the combination of physical and chemical adsorption since the obtained n value is close to the realm of chemical adsorption. The physical adsorption mechanism is directly associated with the multilayer adsorption on adsorbate which is compatible with the Freundlich isotherm theorem, whereas the chemical adsorption is single layer adsorption [85].

Temkin isotherm model claims that the heat of adsorption of the molecules located at the surface, decreasing linearly and adsorption is characterized by a uniform distribution of binding energies [66,86]. In the present study, this model was not found as a reliable model representing the methylene blue adsorption isotherm on sesame seed cake, due to relatively low correlation of coefficient value ($R^2 = 0.9264$) and high standard deviation ($\sigma = 3.0433$).

Dubinin–Radushkevich isotherm model gives an insight into the biomass porosity and the adsorption energy [66]. Dubinin–Radushkevich isotherm model had applied to understand that whether the adsorption is controlled by chemical or physical forces [87]. According to Table 10, the correlation of coefficient was not sufficiently high to accept that the adsorption isotherm model was fitted to the experimental data. Nevertheless, the model parameter of the β coefficient was found as 12.784 mol²/kJ² and used to calculate the free energy of the adsorption process (E) by using the following equation; $E = 1/\sqrt{2\beta}$ and the E was found as 0.198 kJ/mol. According to the literature, the lower value of free energy than 8 kJ/mol is associated with physisorption mechanism of adsorption [5]. Even if the Dubinin–Radushkevich isotherm could not be used as a reliable isotherm model for the present study, the free energy of the adsorption process calculated pointed out that the adsorption process could be controlled in order of physical adsorption.

3.5. Thermodynamic studies on adsorption process

The thermodynamic parameters for instance; free Gibbs energy (ΔG°), enthalpy (ΔH°), and entropy (ΔS°), were evaluated to understand the spontaneity and nature of methylene blue adsorption on sesame seed cake. The following equations (Eqs. (5)–(7)) were used to calculate the thermodynamic parameters [1,18]. In these equations, C_{solid} (mg/L) and C_{liquid} (mg/L) values represent the dye concentration in the solid and liquid phase, respectively.

$$\ln K_c = \frac{\Delta S^\circ}{R} - \frac{\Delta H^\circ}{RT} \tag{5}$$

$$K_c = \frac{C_{solid}}{C_{liquid}} \tag{6}$$

$$\Delta G^\circ = -RT \ln K_c \tag{7}$$

where T is the temperature in Kelvin and R is the gas constant (8.314 J/mol K). In the present study, the temperature dependence of the adsorption process was studied by varying the temperature from 20°C to 40°C (at pH of 9 and adsorbent dosage of 2 g/100 mL with 200 mg/L methylene initial concentration). The varying temperature did not cause any noticeable change in the removal percentage of methylene blue just as this parameter was

found as a less significant parameter compared to pH and adsorbent dosage.

The plot of $\ln(K_c)$ vs. $1/T$ gave the straight line (Fig. 14a), and the values of $\Delta H°$ and $\Delta S°$ were calculated from the slope and intercept of the straight line. Additionally, the $\Delta G°$ value was calculated using Eq. (6). The data calculated were listed in Table 11. According to the data obtained, the positive value of $\Delta H°$ and $\Delta S°$ indicated that the adsorption had an endothermic nature, and the randomness at the solid-solute interface increased during the adsorption [8,88]. In addition, the value of $\Delta H°$ could be used to understand the nature of the adsorption since if the $\Delta H°$ values fell within 1–40 kJ/mol, it indicates physisorption [75]. On the other hand, the negative charge of $\Delta G°$ pointed to that the adsorption process of methylene blue on sesame seed cake was spontaneous at all studied temperatures (293–313 K) [8,12,41].

3.6. Adsorption activation parameters

The activation energy of the methylene blue adsorption on sesame seed cake was calculated by linearized Arrhenius equation given in Eq. (8) [72]:

$$\ln k_2 = \ln A - \frac{E_a}{RT} \tag{8}$$

where E_a is the activation energy (J/mol), k_2 is the rate constant of the pseudo-second-order kinetic model (g/mg min), A is Arrhenius factor, R is the gas constant (8.314 J/mol K), and T is the temperature (K). The magnitude of E_a value gives information about the type of adsorption. According to the literature, the E_a value is in the range between 5 and 40 kJ/mol points out physical adsorption, while the E_a for chemical adsorption falls in the range between 40 and 800 kJ/mol [88,89]. In the present study, the pseudo-second-order rate constant k_2 values obtained at various temperatures were used to plot $\ln k_2$ vs. $1/T$ (Fig. 14b). E_a value was calculated using the given plot in Fig. 14b. The magnitude of E_a was calculated as 8.708 kJ/mol with the correlation coefficient of $R^2 = 0.9995$ and the standard deviation of $\sigma = 0.0037$. The magnitude of E_a indicated that methylene blue adsorption on sesame seed cake was physisorption.

Eventually, the comprehensive studies applied to evaluate the nature of possible interactions between sesame seed cake and methylene blue, the adsorption kinetics, the adsorption isotherm, and adsorption thermodynamic studies revealed that the adsorption of methylene blue on sesame seed cake could involve complex interactions characterized by both of physical and chemical adsorption. Thus, this situation could be explained that the physical adsorption took place on the chemical adsorption monolayer of the adsorbent surface. Additionally, the comprehensive literature survey performed on methylene blue adsorption on the low-cost agricultural wastes were listed in Table 12 to compare the present study with them.

3.7. Reusability performance of sesame seed cake

The reusability performance of sesame seed cake was evaluated since it is a critical point to confirm the stable adsorbent activity in industrial applications. In the present study, the reusability studies were carried out in three subsequent cycles at the already determined optimum

Table 11
Thermodynamic parameters of methylene blue adsorption on sesame seed cake

$\Delta H°$ (J/mol)	$\Delta S°$ (J/mol)	$\Delta G°$ (J/mol)		
		293 K	303 K	313 K
332.27	21.74	–6,036.65	–6,048.59	–6,057.46

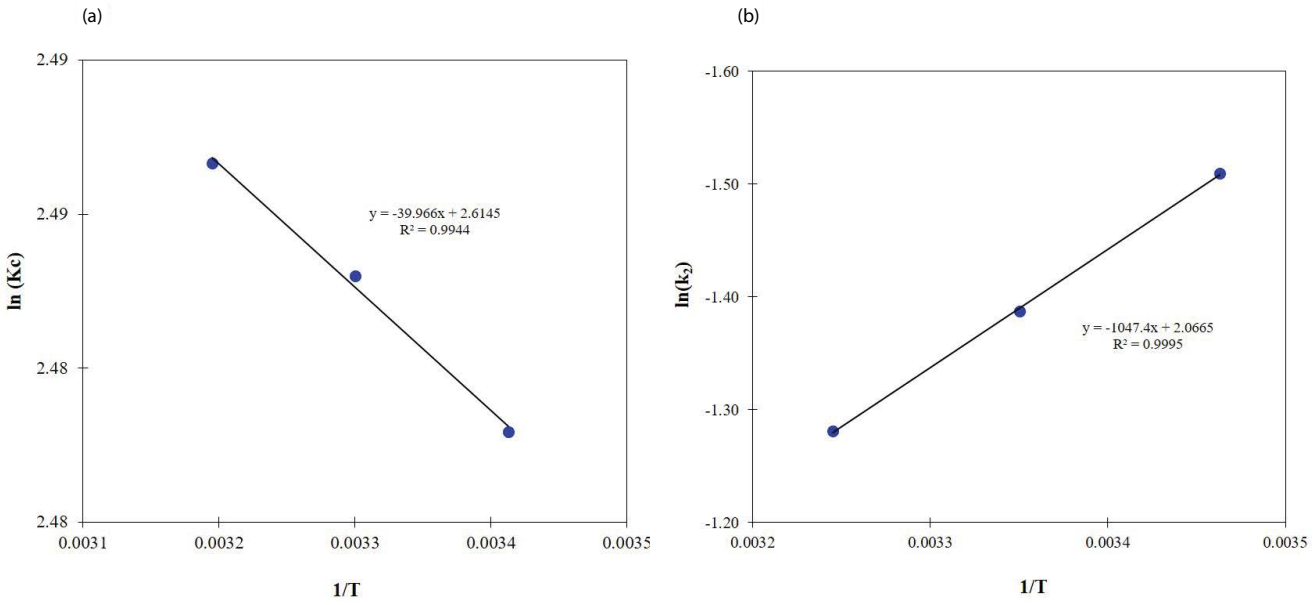

Fig. 14. (a) Plot of $\ln(K_c)$ vs. $1/T$ and (b) Arrhenius plot for methylene blue adsorption on sesame seed cake.

Table 12
Comparison of the several studies reported in the literature for methylene blue adsorption onto various agricultural wastes

Reference	Adsorbent	Process variables						Maximum adsorption capacity (q_m, mg/g)	Adsorption isotherm model	Adsorption kinetic model
		Adsorbent amount (g/L)	Initial dye concentration (mg/L)	Time (min)	Temperature (°C)	pH	Maximum dye removal (%)			
[38]	Rosewood sawdust (pretreated)	2–10	50–250	15–120	26	2–10	99.9	–	–	Pseudo-first-order
[39]	Neem leaf powder	2–10	25–70	60–300	27–67	2–10	95.2	19.61	Freundlich	Pseudo-first-order
[40]	Wheat shells	0.5	200	75	30–50	2–9	95	21.50	Langmuir	Pseudo-second-order
[17]	Bamboo-based activated carbon	1	100–500	48 h	30	7	–	454.2	Langmuir	Pseudo-second-order
[11]	Activated carbon prepared from rattan sawdust	1	100–500	24 h	30	–	–	294.12	Langmuir	Pseudo-second-order
[41]	Activated carbon prepared from sunflower oil cake	0.4	25	1,440	15–45	3–10	–	16.43	Langmuir	Pseudo-second-order
[14]	Spent coffee grounds	5–30	50–500	15–720	25	3–11	99	23	Temkin	Pseudo-second-order
[42]	Pineapple peel powder	1–5	60–100	5–30	25	2–12	–	78.125	Langmuir	Pseudo-second-order
[43]	Tunisian activated carbon	0.2	300	24	25	3–9	–	147	Langmuir	Pseudo-second-order
[19]	Activated carbon produced from flamboyant pods	1	100–1,000	150	25	2–10	90	889.58	Toth	Avrami
[27]	Activated carbon prepared from *Posidonia oceanica* dead leaves	10	250–750	360	25	3–10	–	270.3	Langmuir	Pseudo-second-order
[44]	Activated carbon prepared from cashew nut shell as	0.5–3	50–250	60–120	30	2–10	–	294.12	Redlich–Peterson	Pseudo-second-order
[45]	Papaya leaf powder	0.5–7	50–150	–	–	2.2–10.2	98.8	512.55	Langmuir	Pseudo-second-order
[4]	Carbonized *Parthenium hysterophorus*	0.22–0.5	25–50	60–180	35	5–9	97.8	98.06	Langmuir	Pseudo-second-order
[8]	Pine tree leaves	0.01–0.03	10–90	100	30–60	2.05–9.2	98.7	126.58	Langmuir	Pseudo-second-order
[46]	Field debris of chickpea	1–10	300	10–240	20–50	3–9	–	108.7	Freundlich	Pseudo-second-order
[47]	Activated carbon prepared from pineapple	2	–	120	–	–	99.48	–	–	–
[48]	Corn husk	0.5	5–30	120	25–28	2–10	90	30.33	Langmuir	Pseudo-second-order
[21]	Oil palm leaves	0.25–2.5	50–400	40	30–70	2–8	88.72	103.02	Freundlich	Pseudo-second-order
[20]	Activated carbon produced from *Ficus carica* bast	1–9	100–900	10–90	25–50	2–12	95	47.62	Langmuir	Pseudo-second-order and intraparticle diffusion model
[1]	Walnut shells powder	0.5–2	20–100	120	20–50	4–12	90	178.9	Langmuir	Pseudo-second-order
[49]	Corncob	10	2.5–20	10–1,440	10–30	2–10	99.90	417.12	Langmuir	Pseudo-second-order
[50]	Ginger straw waste derived porous carbons	1	100	60	25	2–12	–	62.54	Langmuir	Pseudo-second-order
[51]	Activated carbon prepared from *Citrus limetta* peels	1–5	100–500	10–90	28	1–9	84	500	Langmuir	Elovich
[52]	Silica derived from the raw rice husk	0.5–2	10–100	30–90	–	5–9	96.7	103.11	Langmuir	–
Present Study	Sesame seed cake	10–30	200	25	20–40	3–9	94.18	108.69	Freundlich	Pseudo-second-order

point of the adsorption process (temperature of 20°C, pH of 9, an adsorbent dosage of 2 g/100 mL) with 100 mg/mL initial methylene blue concentration. The procedure was applied similarly according to the previous work reported by Jain et al. [65]. After the first adsorption process, the dye laden adsorbent was separated from the media, and desorption study was performed by using ethanol as desorption and regeneration agent. For this purpose, dye laden adsorbent was mixed with ethanol and stirred in a shaker for 25 min and subsequently, the regenerated adsorbent was again used for adsorption. The results were expressed as an average of three replication with ±5% reproducibility of the results. The percentage of desorption was calculated as a ratio of the concentration of dye in the desorbed phase and adsorbed phase [71].

According to the data obtained (Fig. 15), the efficient desorption could not be achieved most probably because of the presence of strong hydrogen bonds, π–π interactions, *n*–π interactions, and also electrochemical interactions between methylene blue and sesame seed cake as revealed by FTIR analysis. Thus, the inefficient desorption percentage could be acceptable, since the adsorption mechanism of methylene blue was determined as a complex process involving both of the physical and chemical interactions that took place at the surface and interior of the sesame seed cake pores with a contribution of film diffusion, as described previously.

Here in, it is worth commenting on the coefficients such as R_L (0.45) and β (2.8425 g/mg) obtained from the Langmuir isotherm and Elovich kinetic model equations, even if they were not accepted as the most appropriate model describing the methylene blue adsorption on sesame seed cake. As mentioned previously, the R_L represented the theoretical separation factor and nearly close zero R_L values meant that the adsorption process was nearly irreversible. Additionally, it was already concluded that the adsorption of methylene blue on sesame seed cake had higher potential than desorption since the found β value (2.8425 g/mg) was less than α (26.6273 mg/g min). In the light of these findings, it could be a wise expectation that the methylene blue could not fully desorb from the sesame seed cake.

The desorption of methylene blue was found as approximately 45% for the first cycle whereas it was found as approximately 30% for the third cycle. The decrease of the desorption capacity could be explained by the newly formed strong hydrogen bonds between the methylene blue and regenerated sesame seed cake. Although the desorption performance of sesame seed cake was not found as satisfying, the adsorption capacity of the regenerated sesame seed cake was slightly reduced from approximately 92% to 89%. This situation could be attributed to the formation of active OH^- sites that came from the ethanol regeneration and the contribution of these groups in the new formation of strong hydrogen bonds between the methylene blue and sesame seed cake. As a result, the sesame seed cake is a readily reusable adsorbent for methylene blue adsorption without any significant drop in its adsorption capacity even if its desorption percentage was highly low.

4. Conclusions

In the present study; low-cost agricultural waste, sesame seed cake without applying any pretreatment techniques, was utilized as an adsorbent for methylene blue adsorption in a very short time (25 min) and structural, morphological, and chemical properties of sesame seed cake were characterized by FTIR, SEM/EDX, and BET analysis. The characterization studies enlightened that the sesame seed cake had various functional groups involved in the adsorption process. The adsorption process was optimized by RSM, BBD by using three independent process variables (pH, adsorbent dosage, and temperature), and the results

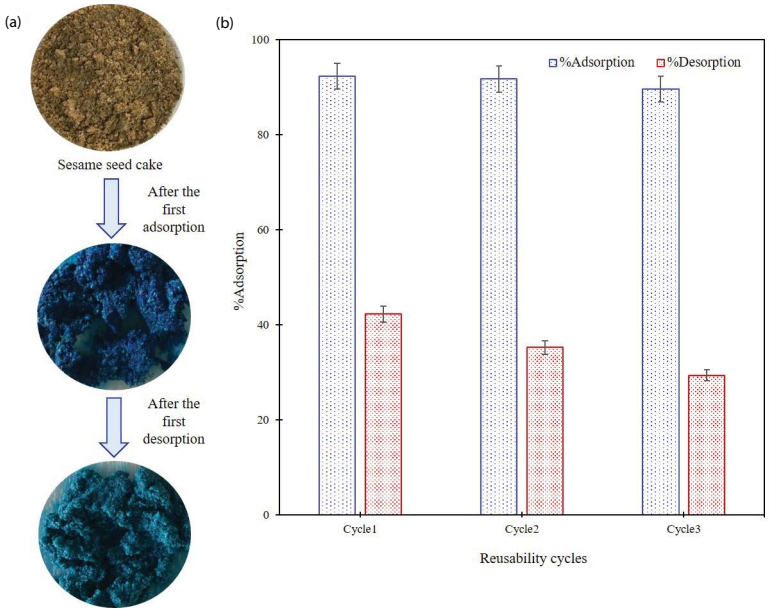

Fig. 15. (a) Physical change and (b) reusability cycles of sesame seed cake.

were evaluated by ANOVA analysis. The findings were summarized given as follows:

- The quadratic mathematical model was developed to describe the response behavior by varying the operating conditions since the *F*-value of the model was found as large as indicating the model significance. Three independent process variables individual effects to methylene blue removal on sesame seed cake was ordered as pH > adsorbent dosage > temperature.
- The characterization studies revealed that electrostatic, n–π and π–π interactions and hydrogen bonding had played a significant role in the adsorption process.
- The comprehensive adsorption kinetic, isotherm, and thermodynamic studies were conducted to reveal the complex adsorption mechanism of methylene blue on sesame seed cake, involved both physical and chemical interactions. These results showed that the methylene blue adsorption on sesame seed cake followed the pseudo-second-order kinetic model and Freundlich isotherm model, respectively.
- The reusability studies indicated that sesame seed cake was a regenerable substance keeping the adsorption capacity in three cycles, even if desorption of methylene blue percentage was not satisfying due to the nature of the adsorption process.

References

[1] Y. Miyah, A. Lahrichi, M. Idrissi, A. Khalil, F. Zerrouq, Adsorption of methylene blue dye from aqueous solutions onto walnut shells powder: equilibrium and kinetic studies, Surf. Interfaces, 11 (2018) 74–81.

[2] T. Rasheed, M. Bilal, F. Nabeel, M. Adeel, H.M.N. Iqbal, Environmentally-related contaminants of high concern: potential sources and analytical modalities for detection, quantification, and treatment, Environ. Int., 122 (2019) 52–66.

[3] C.A. Igwegbe, L. Mohmmadi, S. Ahmadi, A. Rahdar, D. Khadkhodaiy, R. Dehghani, S. Rahdar, Modeling of adsorption of Methylene Blue dye on Ho-$CaWO_4$ nanoparticles using response surface methodology (RSM) and artificial neural network (ANN) techniques, MethodsX, 6 (2019) 1779–1797.

[4] S. Chatterjee, A. Kumar, S. Basu, S. Dutta, Application of response surface methodology for methylene blue dye removal from aqueous solution using low cost adsorbent, Chem. Eng. J., 181–182 (2012) 289–299.

[5] D. Allouss, Y. Essamlali, O. Amadine, A. Chakir, M. Zahouily, Response surface methodology for optimization of methylene blue adsorption onto carboxymethyl cellulose-based hydrogel beads: adsorption kinetics, isotherm, thermodynamics and reusability studies, RSC Adv., 9 (2019) 37858–37869.

[6] S. Dutta, A. Bhattacharyya, A. Ganguly, S. Gupta, S. Basu, Application of response surface methodology for preparation of low-cost adsorbent from citrus fruit peel and for removal of Methylene Blue, Desalination, 275 (2011) 26–36.

[7] M. Rafatullah, O. Sulaiman, R. Hashim, A. Ahmad, Adsorption of methylene blue on low-cost adsorbents: a review, J. Hazard. Mater., 177 (2010) 70–80.

[8] M.T. Yagub, T.K. Sen, H.M. Ang, Equilibrium, kinetics, and thermodynamics of methylene blue adsorption by pine tree leaves, Water Air Soil Pollut., 223 (2012) 5267–5282.

[9] B.H. Hameed, A.A. Ahmad, Batch adsorption of methylene blue from aqueous solution by garlic peel, an agricultural waste biomass, J. Hazard. Mater., 164 (2009) 870–875.

[10] M.C. Somasekhara Reddy, V. Nirmala, C. Ashwini, Bengal gram seed husk as an adsorbent for the removal of dye from aqueous solutions – Batch studies, Arabian J. Chem., 10 (2017) S2554–S2566.

[11] B.H. Hameed, A.L. Ahmad, K.N.A. Latiff, Adsorption of basic dye (methylene blue) onto activated carbon prepared from rattan sawdust, Dyes Pigm., 75 (2007) 143–149.

[12] L. Mouni, L. Belkhiri, J.C. Bollinger, A. Bouzaza, A. Assadi, A. Tirri, F. Dahmoune, K. Madani, H. Remini, Removal of methylene blue from aqueous solutions by adsorption on kaolin: kinetic and equilibrium studies, Appl. Clay Sci., 153 (2018) 38–45.

[13] M.A.M. Salleh, D.K. Mahmoud, W.A.W.A. Karim, A. Idris, Cationic and anionic dye adsorption by agricultural solid wastes: a comprehensive review, Desalination, 280 (2011) 1–13.

[14] A.S. Franca, L.S. Oliveira, M.E. Ferreira, Kinetics and equilibrium studies of methylene blue adsorption by spent coffee grounds, Desalination, 249 (2009) 267–272.

[15] M. Vakili, M. Rafatullah, B. Salamatinia, A.Z. Abdullah, M.H. Ibrahim, K.B. Tan, Z. Gholami, P. Amouzgar, Application of chitosan and its derivatives as adsorbents for dye removal from water and wastewater: a review, Carbohydr. Polym., 113 (2014) 115–130.

[16] M.T. Yagub, T.K. Sen, S. Afroze, H.M. Ang, Dye and its removal from aqueous solution by adsorption: a review, Adv. Colloid Interface Sci., 209 (2014) 172–184.

[17] B. Hameed, A. Dın, A. Ahmad, Adsorption of methylene blue onto bamboo-based activated carbon: kinetics and equilibrium studies, J. Hazard. Mater., 141 (2007) 819–825.

[18] P.M.K. Reddy, P. Verma, C. Subrahmanyam, Bio-waste derived adsorbent material for methylene blue adsorption, J. Taiwan Inst. Chem. Eng., 58 (2015) 500–508.

[19] A.M.M. Vargas, A.L. Cazetta, M.H. Kunita, T.L. Silva, V.C. Almeida, Adsorption of methylene blue on activated carbon produced from flamboyant pods (*Delonix regia*): study of adsorption isotherms and kinetic models, Chem. Eng. J., 168 (2011) 722–730.

[20] D. Pathania, S. Sharma, P. Singh, Removal of methylene blue by adsorption onto activated carbon developed from *Ficus carica* bast, Arabian J. Chem., 10 (2017) S1445–S1451.

[21] H.D. Setiabudi, R. Jusoh, S.F.R.M. Suhaimi, S.F. Masrur, Adsorption of methylene blue onto oil palm (*Elaeis guineensis*) leaves: process optimization, isotherm, kinetics and thermodynamic studies, J. Taiwan Inst. Chem. Eng., 63 (2016) 363–370.

[22] M.A. Ahmad, N.K. Rahman, Equilibrium, kinetics and thermodynamic of Remazol Brilliant Orange 3R dye adsorption on coffee husk-based activated carbon, Chem. Eng. J., 170 (2011) 154–161.

[23] Y.L. Cao, Z.H. Pan, Q.X. Shi, J.Y. Yu, Modification of chitin with high adsorption capacity for methylene blue removal, Int. J. Biol. Macromol., 114 (2018) 392–399.

[24] M. Naushad, G. Sharma, Z.A. Alothman, Photodegradation of toxic dye using Gum Arabic-crosslinked-poly(acrylamide)/$Ni(OH)_2$/FeOOH nanocomposites hydrogel, J. Cleaner Prod., 241 (2019) 1–9, doi: 10.1016/j.jclepro.2019.118263.

[25] M.J. Iqbal, M.N. Ashiq, Adsorption of dyes from aqueous solutions on activated charcoal, J. Hazard. Mater., 139 (2007) 57–66.

[26] I. Anastopoulos, G.Z. Kyzas, Agricultural peels for dye adsorption: a review of recent literature, J. Mol. Liq., 200 (2014) 381–389.

[27] M.U. Dural, L. Cavas, S.K. Papageorgiou, F.K. Katsaros, Methylene blue adsorption on activated carbon prepared from *Posidonia oceanica* (L.) dead leaves: kinetics and equilibrium studies, Chem. Eng. J., 168 (2011) 77–85.

[28] K. Ravilumar, S. Ramalingam, S. Krishnan, K. Balu, Application of response surface methodology to optimize the process variables for Reactive Red and Acid Brown dye removal using a novel adsorbent, Dyes Pigm., 70 (2006) 18–26.

[29] R. Rajeshkannan, N. Rajamohan, M. Rajasimman, Removal of malachite green from aqueous solution by sorption on hydrilla verticillata biomass using response surface methodology, Front. Chem. Eng. China, 3 (2009) 146–154.

[30] S. Karimifard, M.R. Alavi Moghaddam, Application of response surface methodology in physicochemical removal

of dyes from wastewater: a critical review, Sci. Total Environ., 640–641 (2018) 772–797.
[31] M. Mourabet, A. El Rhilassi, H. El Boujaady, M. Bennani-Ziatni, A. Taitai, Use of response surface methodology for optimization of fluoride adsorption in an aqueous solution by Brushite, Arabian J. Chem., 10 (2017) S3292–S3302.
[32] J.U. Ani, U.C. Okoro, L.E. Aneke, O.D. Onukwuli, I.O. Obi, K.G. Akpomie, A.C. Ofomatah, Application of response surface methodology for optimization of dissolved solids adsorption by activated coal, Appl. Water Sci., 9 (2019) 1–11.
[33] G. Annadurai, R.Y. Sheeja, Use of Box–Behnken design of experiments for the adsorption of vetofix red using biopolymer, Bioprocess Eng., 18 (1998) 463–466.
[34] M. Moradi, M. Fazlzadehdavil, M. Pirsaheb, Y. Mansouri, T. Khosravi, K. Sharafi, Response surface methodology (RSM) and its application for optimization of ammonium ions removal from aqueous solutions by pumice as a natural and low cost adsorbent, Arch. Environ. Prot., 42 (2016) 33–43.
[35] R. Zhou, M. Zhang, J. Zhou, J. Wang, Optimization of biochar preparation from the stem of *Eichhornia crassipes* using response surface methodology on adsorption of Cd^{2+}, Sci. Rep., 9 (2019) 1–17.
[36] M.A. Bezerra, R.E. Santelli, E.P. Oliveira, L.S. Villar, L.A. Escaleira, Response surface methodology (RSM) as a tool for optimization in analytical chemistry, Talanta, 76 (2008) 965–977.
[37] S. Rangabhashiyam, M.S. Giri Nandagopal, E. Nakkeeran, R. Keerthi, N. Selvaraju, Use of Box–Behnken design of experiments for the adsorption of chromium using immobilized macroalgae, Desal. Water Treat., 57 (2016) 26101–26113.
[38] V.K. Garg, M. Amita, R. Kumar, R. Gupta, Basic dye (methylene blue) removal from simulated wastewater by adsorption using Indian Rosewood sawdust: a timber industry waste, Dyes Pigm., 63 (2004) 243–250.
[39] K.G. Bhattacharya, A. Sharma, Kinetics and thermodynamics of Methylene Blue adsorption on Neem (*Azadirachta indica*) leaf powder, Dyes Pigm., 65 (2005) 51–59.
[40] Y. Bulut, H. Aydin, A kinetics and thermodynamics study of methylene blue adsorption on wheat shells, Desalination, 194 (2006) 259–267.
[41] S. Karagöz, T. Tay, S. Ucar, M. Erdem, Activated carbons from waste biomass by sulfuric acid activation and their use on methylene blue adsorption, Bioresour. Technol., 99 (2008) 6214–6222.
[42] N.A. Lutpi, T.H. Yin, W.Y. Shian, A.N. Kamarudzaman, Removal of Methylene Blue Using Pineapple Peel Powder as Adsorbent, Proceedings of the 3rd CUTSE International Conference Miri, Sarawak, Malaysia, 2011, pp. 352–356.
[43] A. Kriaa, N. Hamdi, E. Srasra, Adsorption studies of methylene blue dye on Tunisian activated lignin, Russ. J. Phys. Chem. A, 85 (2011) 279–287.
[44] P.S. Kumar, S. Ramalingam, K. Sathishkumar, Removal of methylene blue dye from aqueous solution by activated carbon prepared from cashew nut shell as a new low-cost adsorbent, Korean J. Chem. Eng., 28 (2011) 149–155.
[45] M.Z. Bin Mukhlish, M.R. Khan, M.C. Bhoumick, S. Paul, Papaya (*Carica papaya* L.) leaf powder: novel adsorbent for removal of methylene blue from aqueous solution, Water Air Soil Pollut., 223 (2012) 4949–4958.
[46] M. Kiliç, G. Özsin, B.B. Uzun, A.E. Pütün, Ö. Çepelioğullar, Nohut samanı tarla atığının sulu çözeltilerden metilen mavisi gideriminde düşük maliyetli biyosorbent olarak değerlendirilmesi, J. Fac. Eng. Archit. Gazi Univ., 29 (2014) 717–726.
[47] N. Selvanathan, N.S. Subki, Dye adsorbent by pineapple activated carbon: H_3PO_4 and NaOH activation, ARPN J. Eng. Appl. Sci., 10 (2015) 9476–9480.
[48] D.S. Malik, C.K. Jain, A.K. Yadav, R. Kothari, V. V Pathak, Removal of methylene blue dye in aqueous solution by agricultural waste, Int. Res. J. Eng. Technol., 3 (2016) 1–17.
[49] H.J. Choi, S.W. Yu, Biosorption of methylene blue from aqueous solution by agricultural bioadsorbent corncob, Environ. Eng. Res., 24 (2019) 99–106.
[50] W. Zhang, H. Li, J. Tang, H. Lu, Y. Liu, Ginger straw waste-derived porous carbons as effective adsorbents toward methylene blue, Molecules, 24 (2019) 1–8.
[51] S. Singh, G.K. Sidhu, H. Singh, Removal of methylene blue dye using activated carbon prepared from biowaste precursor, Indian Chem. Eng., 61 (2019) 28–39.
[52] K. Moeinian, S.M. Mehdinia, Removing methylene blue from aqueous solutions using rice husk silica adsorbent, Polish J. Environ. Stud., 28 (2019) 2281–2288.
[53] S. Akhouairi, H. Ouachtak, A.A. Addi, A. Jada, J. Douch, Natural sawdust as adsorbent for the Eriochrome Black T dye removal from aqueous solution, Water Air Soil Pollut., 230 (2019) 1–15, doi: 10.1007/s11270-019-4234-6.
[54] M.A.P. Gawbah, A.A. Elbadawi, Y.A. Alsabah, M.U. Orsod, A.A.S. Marouf, Characterization of the crystal structure of sesame seed cake burned by Nd: YAG Laser, J. Mater. Sci. Chem. Eng., 6 (2018) 121–131.
[55] H.N. Tran, Y.F. Wang, S.J. You, H.P. Chao, Insights into the mechanism of cationic dye adsorption on activated charcoal: the importance of Π–Π interactions, Process Saf. Environ. Prot., 107 (2017) 168–180.
[56] S.N. Jain, V.B. Garud, S.D. Dawange, D.D. Sonawane, E.R. Shaikh, Sesame (*Sesamum indicum*) oil cake—industrial waste biomass for sequestration of Basic Blue 26 from aqueous media, Biomass Convers. Biorefin., 10 (2020) 1–12, doi: 10.1007/s13399-020-00881-0.
[57] O.V. Ovchinnikov, A.V. Evtukhova, T.S. Kondratenko, M.S. Smirnov, V.Y. Khokhlov, O.V. Erina, Manifestation of intermolecular interactions in FTIR spectra of methylene blue molecules, Vib. Spectrosc., 86 (2016) 181–189.
[58] A.E. Segneanu, I. Gozescu, A. Dabici, P. Sfirloaga, Z. Szabadai, Organic Compounds FT-IR Spectroscopy, J. Uddin, Ed., Macro To Nano Spectroscopy, InTech, 2012, pp. 145–163. Available at: https://www.intechopen.com/books/macro-to-nano-spectroscopy/organic-compounds-ft-ir-spectroscopy
[59] V.P. Dinh, T.D.T. Huynh, H.M. Le, V.D. Nguyen, V.A. Dao, N.Q. Hung, L.A. Tuyen, S. Lee, J. Yi, T.D. Nguyen, L.V. Tan, Insight into the adsorption mechanisms of methylene blue and chromium(III) from aqueous solution onto pomelo fruit peel, RSC Adv., 9 (2019) 25847–25860.
[60] J.B. Lambert, Introduction to Organic Spectroscopy, Macmillan, New York, NY, 1987.
[61] G. Socrates, Infrared and Raman Characteristic Group Frequencies: Tables and Charts, in: Infrared Raman Characteristic Group Frequency, Wiley Editorial Office, Chichester, 2001, pp. 140–343.
[62] S. Sahu, S. Pahi, S. Tripathy, S.K. Singh, A. Behera, U.K. Sahu, R.K. Patel, Adsorption of methylene blue on chemically modified lychee seed biochar: dynamic, equilibrium, and thermodynamic study, J. Mol. Liq., 315 (2020) 1–11, doi: 10.1016/j.molliq.2020.113743.
[63] H.N. Tran, S.J. You, H.P. Chao, Insight into adsorption mechanism of cationic dye onto agricultural residues-derived hydrochars: negligible role of π–π interaction, Korean J. Chem. Eng., 34 (2017) 1708–1720.
[64] R. El Haouti, H. Ouachtak, A. El Guerdaoui, A. Amedlous, E. Amaterz, R. Haounati, A.A. Addi, F. Akbal, N. El Alem, M.L. Taha, Cationic dyes adsorption by Na-montmorillonite nano clay: experimental study combined with a theoretical investigation using DFT-based descriptors and molecular dynamics simulations, J. Mol. Liq., 290 (2019) 1–15, doi: 10.1016/j.molliq.2019.111139.
[65] S.N. Jain, S.R. Tamboli, D.S. Sutar, S.R. Jadhav, J.V. Marathe, A.A. Shaikh, A.A. Prajapati, Batch and continuous studies for adsorption of anionic dye onto waste tea residue: kinetic, equilibrium, breakthrough and reusability studies, J. Cleaner Prod., 252 (2020) 1–15, doi: 10.1016/j.jclepro.2019.119778.
[66] A.A. Inyinbor, F.A. Adekola, G.A. Olatunji, Kinetics, isotherms and thermodynamic modeling of liquid phase adsorption of Rhodamine B dye onto Raphia hookerie fruit epicarp, Water Resour. Ind., 15 (2016) 14–27.
[67] F. Largo, R. Haounati, S. Akhouairi, H. Ouachtak, R. El Haouti, A. El Guerdaoui, N. Hafid, D.M.F. Santos, F. Akbal, A. Kuleyin,

A. Jada, A.A. Addi, Adsorptive removal of both cationic and anionic dyes by using sepiolite clay mineral as adsorbent: experimental and molecular dynamic simulation studies, J. Mol. Liq., 318 (2020) 1–14, doi: 10.1016/j.molliq.2020.114247.
[68] B. Sadhukhan, N.K. Mondal, S. Chattoraj, Optimisation using central composite design (CCD) and the desirability function for sorption of methylene blue from aqueous solution onto Lemna major, Karbala Int. J. Mod. Sci., 2 (2016) 145–155.
[69] M. Pirsaheb, Z. Rezai, A.M. Mansouri, A. Rastegar, A. Alahabadi, A.R. Sani, K. Sharafi, Preparation of the activated carbon from India shrub wood and their application for methylene blue removal: modeling and optimization, Desal. Water Treat., 57 (2016) 5888–5902.
[70] S. Chattoraj, N.K. Mondal, B. Sadhukhan, P. Roy, T.K. Roy, Optimization of adsorption parameters for removal of carbaryl ınsecticide using neem bark dust by response surface methodology, Water Conserv. Sci. Eng., 1 (2016) 127–141.
[71] A.B. Albadarin, M.N. Collins, M. Naushad, S. Shirazian, G. Walker, C. Mangwandi, Activated lignin-chitosan extruded blends for efficient adsorption of methylene blue, Chem. Eng. J., 307 (2017) 264–272.
[72] M. Doğan, Y. Özdemir, M. Alkan, Adsorption kinetics and mechanism of cationic methyl violet and methylene blue dyes onto sepiolite, Dyes Pigm., 75 (2007) 701–713.
[73] J. Goscianska, N.A. Fathy, R.M.M. Aboelenin, Adsorption of solophenyl red 3BL polyazo dye onto amine-functionalized mesoporous carbons, J. Colloid Interface Sci., 505 (2017) 593–604.
[74] H. Ouachtak, R. El Haouti, A. El Guerdaoui, R. Haounati, E. Amaterz, A.A. Addi, F. Akbal, M.L. Taha, Experimental and molecular dynamics simulation study on the adsorption of Rhodamine B dye on magnetic montmorillonite composite γ-Fe_2O_3@Mt, J. Mol. Liq., 309 (2020) 1–17, doi: 10.1016/j.molliq.2020.113142.
[75] T.C. Egbosiuba, A.S. Abdulkareem, A.S. Kovo, E.A. Afolabi, J.O. Tijani, M. Auta, W.D. Roos, Chemical engineering research and design ultrasonic enhanced adsorption of methylene blue onto the optimized surface area of activated carbon : adsorption isotherm, kinetics and thermodynamics, Chem. Eng. Res. Des., 153 (2019) 315–336.
[76] M. Pooresmaeil, H. Namazi, Application of Polysaccharide-Based Hydrogels for Water Treatments, Elsevier Inc., Beijing, P.R. China, 2019.
[77] S. Karimi, M. Tavakkoli Yaraki, R.R. Karri, A comprehensive review of the adsorption mechanisms and factors influencing the adsorption process from the perspective of bioethanol dehydration, Renewable Sustainable Energy Rev., 107 (2019) 535–553.
[78] S. Karthikeyan, B. Sivakumar, N. Sivakumar, Film and pore diffusion modeling for adsorption of reactive red 2 from aqueous solution on to activated carbon prepared from bio-diesel industrial waste, E-J. Chem., 7 (2010) 175–185.
[79] S. Chowdhury, R. Mishra, P. Saha, P. Kushwaha, Adsorption thermodynamics, kinetics and isosteric heat of adsorption of malachite green onto chemically modified rice husk, Desalination, 265 (2011) 159–168.
[80] S. Nethaji, A. Sivasamy, A.B. Mandal, Adsorption isotherms, kinetics and mechanism for the adsorption of cationic and anionic dyes onto carbonaceous particles prepared from *Juglans regia* shell biomass, Int. J. Environ. Sci. Technol., 10 (2013) 231–242.
[81] P. Parthasarathy, S.K. Narayanan, Effect of hydrothermal carbonization reaction parameters on the properties of hydrochar and pellets, Environ. Prog. Sustainable Energy, 33 (2014) 676–680.
[82] J.M. Salman, V.O. Njoku, B.H. Hameed, Bentazon and carbofuran adsorption onto date seed activated carbon: kinetics and equilibrium, Chem. Eng. J., 173 (2011) 361–368.
[83] M.B. Desta, Batch sorption experiments: Langmuir and Freundlich ısotherm studies for the adsorption of textile metal ıons onto teff straw (*Eragrostis tef*) agricultural waste, J. Thermodyn., 2013 (2013) 1–6.
[84] M. Asgari, H. Anisi, H. Mohammadi, S. Sadighi, Designing a commercial scale pressure swing adsorber for hydrogen purification, Pet. Coal., 56 (2014) 552–561.
[85] V. Adsorption, C. Equipped, P. Membrane, Application of Freundlich and Temkin ısotherm to study the removal of Pb(II) via adsorption on activated carbon equipped polysulfone membrane, Int. J. Eng. Technol., 7 (2018) 91–93.
[86] D. Kavitha, C. Namasivayam, Experimental and kinetic studies on methylene blue adsorption by coir pith carbon, Bioresour. Technol., 98 (2007) 14–21.
[87] Q. Hu, Z. Zhang, Application of Dubinin–Radushkevich isotherm model at the solid/solution interface: a theoretical analysis, J. Mol. Liq., 277 (2019) 646–648.
[88] Y. Zhang, F. Yu, W. Cheng, J. Wang, J. Ma, Adsorption equilibrium and kinetics of the removal of ammoniacal nitrogen by zeolite X/activated carbon composite synthesized from elutrilithe, J. Chem., 2017 (2017) 1–9.
[89] J. Wu, A. Xia, C. Chen, L. Feng, X. Su, X. Wang, Adsorption thermodynamics and dynamics of three typical dyes onto bio-adsorbent spent substrate of *Pleurotus eryngii*, Int. J. Environ. Res. Public Health, 16 (2019) 1–11, doi: 10.3390/ijerph16050679.